https://doi.org/10.5194/hess-2024-37
Preprint. Discussion started: 20 February 2024

Hydrology and Earth System Sciences
Discussions

Green water availability and water-limited crop yields under a changing climate in Ethiopia

Mosisa Tujuba Wakjira[1], Nadav Peleg[2], Johan Six[3], Peter Molnar[1]

[1]Institute of Environmental Engineering, ETH Zurich, Laura-Hezner-Weg 7, CH-8093 Zürich, Switzerland
[2]Institute of Earth Surface Dynamics, University of Lausanne, CH-1015 Lausanne, Switzerland
[3]Institute of Agricultural Science, ETH Zurich, Universitätstrasse 2, CH-8092 Zürich, Switzerland

Correspondence to: Mosisa Tujuba Wakjira (wakjira@ifu.baug.ethz.ch; mosisatujuba@gmail.com)

Abstract. Climate change is expected to influence future agricultural water availability, posing particular challenges in rainfed agricultural systems. This study aims to analyze the climatology of green water availability and water-limited attainable yields (AY) – the maximum crop yield achieved with available green water under optimal soil nutrient and crop management, considering four major cereal crops (teff, maize, sorghum, and wheat) produced in Ethiopia. An agrohydrological modelling framework was developed to simulate climatic-hydrological-crop interactions. The model was applied to a reference (1981-2010) and future periods (2020-2099) under low, intermediate, and high greenhouse gas emission scenarios in order to: (i) evaluate the current green water availability and AY potential; (ii) assess their climate-driven changes; and (iii) analyze the sensitivity of changes in AY to changes in rainfall and atmospheric evaporative demand. With regional variations based on climatic regimes, the main growing season (Meher, May to September) has an average AY of 79 % of a fully irrigated potential yield with an average soil moisture deficit of 29 % of moisture content at full water holding capacity. AY of the short growing season (Belg, February-May) is on average 37 % of the potential yield, with a soil moisture deficit of 56 %. Under the future climate, Meher is expected to experience small changes in the range of ±5 % with dominantly positive trends in the 2030s and decreases in the 2060s and 2080s, mainly driven by changes in the atmospheric evaporative demand due to rising temperatures. The Belg-producing regions are expected to experience increased AY that is dominantly controlled by increases in rainfall. On the other hand, a substantial yield gap is identified between actual and water-limited yields. This points to the need for combining green water management practices with nutrient and tillage management, plant protection, and cultivar improvement to close the yield gaps and to build up climate resilience of farmers.

1. Introduction

Green water, the infiltrated part of rainfall that is stored in the soil root zone and returns to the atmosphere in the form of evapotranspiration (Falkenmark, 2006), is the sole source of moisture in rainfed agriculture (RFA) systems (Rockström, 1999). Green water accounts for an estimated 80 % of the global agricultural evapotranspiration fluxes, and RFA systems produce ~60 % of the global food (Mekonnen and Hoekstra, 2011; Molden et al., 2011; Rockström et al., 2010; Sposito, 2013). The reliance on green water varies across regions, with sub-Saharan Africa (SSA) being particularly dependent on this water

https://doi.org/10.5194/hess-2024-37
Preprint. Discussion started: 20 February 2024


Hydrology and Earth System Sciences
Discussions

resource, where close to 95 % of croplands are under rainfed agriculture practices (Abrams, 2018; Laderach et al., 2021). Due to the highly dynamic nature of green water availability (GWA), influenced by climatic and biophysical factors that vary in space and time, RFA systems are strongly climate-sensitive under moisture-limited conditions (Kang et al., 2009; Meng et al., 2023; Park et al., 2022). Climate change presents an additional major challenge to the system, undermining crop production with potential consequences of food insecurity, livelihood losses, and economic crises (FAO, 2022).

Previous global-scale assessments have highlighted the challenges posed by climate change on agriculture, both in the past and in the future, leading to regionally varying intensification of agricultural water scarcity and decreases in crop yields (e.g., Borgomeo et al., 2020; Jägermeyr et al., 2021; Lobell et al., 2011; Rosenzweig et al., 2014). This is particularly evident across the tropics including the highly climate-vulnerable SSA countries (Burke et al., 2009; Kummu et al., 2021; Müller et al., 2011; Rezaei et al., 2023; Rosenzweig et al., 2014; Schlenker and Lobell, 2010). Adaptation actions tailored to specific contexts are now a top priority for mitigating the impacts of climate change-induced water scarcity in rainfed agriculture (RFA) systems, primarily at the national scale through the implementation of National Adaptation Plans (NAP) under the auspices of the United Nations Framework Convention on Climate Change (UNFCCC, 2021) and other programs.

Ethiopia is one of the countries committed to formulating and implementing the NAP, including in agriculture, the sector which the country and its population heavily rely on (FDRE, 2019). In fact, climate adaptation is a much-needed action in Ethiopian smallholder agriculture, of which ~95 % is dependent on GWA, and at the same time it is an indispensable activity supporting the food and income of nearly 80 % of the population. The NAP and its implementations are, in principle, based on analyses of climate change impacts and vulnerability, along with relevant adaptation actions (UNFCCC, 2021; Warren et al., 2018). Previous studies on the crop yield impacts of climate change in Ethiopia have mainly focused on local case studies (e.g., Abera et al., 2018; Araya et al., 2015; Degife et al., 2021; Hadgu et al., 2015; Kassie et al., 2014; Markos et al., 2023; Moges and Gangadhara, 2021), making them patchy and insufficient as a comprehensive guide for the NAP. Here we propose a framework which allows for a regional comprehensive analysis of agrohydrological responses to climate change across the RFA regions of Ethiopia.

This framework builds on the key factors that influence GWA and their cascading effects on crop yield, to guide appropriate agricultural water management planning, decisions and actions. Several factors influence GWA. While rainfall amount fundamentally determines the green water supply, rainfall event characteristics such as intensity, frequency, and duration, combined with surface biophysical conditions (mainly soil, land cover, terrain slope, and roughness), govern the partitioning of rainfall into overland flow and infiltration (Rockström and Gordon, 2001; Schuol et al., 2008). Soil properties (e.g., textural composition, organic matter content, thickness, and salinity) in particular determine the rainfall partitioning to infiltration and runoff, the subsurface flow, green water storage capacity, and plant accessibility, while potential evapotranspiration driven by air temperature, radiation, wind, relative humidity, and vegetation controls the return flow of green water to the atmosphere (Ringersma et al., 2003).

https://doi.org/10.5194/hess-2024-37
Preprint. Discussion started: 20 February 2024


Hydrology and Earth System Sciences
Discussions

In moisture-limited regions, crop yield is proportional to the magnitude of the evapotranspiration flux, which is constrained by moisture availability (Hatfield and Dold, 2019; Steduto et al., 2012). The maximum yield that can be achieved with the available green water under the best nutrient input and crop management conditions in RFA systems is considered to be the *water-limited attainable yield* (van Ittersum et al., 2013; Lobell et al., 2009). In conditions where water is not a limiting factor, like in RFA systems in humid agroecologies and fully irrigated systems in dry agroecologies, maximum achievable crop yield is limited by energy, and thus is called *energy-limited yield potential*.

Quantification of the complex interactions between climate, soil, cultivar and crop management is commonly done with mechanistic crop models, for example, APSIM (Holzworth et al., 2014), AquaCrop (Raes et al., 2009; Steduto et al., 2009), CROPSYST (Stöckle et al., 2003), DSSAT (Jones et al., 2003), EPIC (Williams, 1990), and WOFOST (van Diepen et al., 1989), which are used to simulate crop growth and yields at field scale. These models combine hydrological models that simulate hydroclimatic processes to estimate water availability in space and time, and crop growth models that simulate the crop phenological responses to the agro-environmental and management conditions (Siad et al., 2019). Model complexity, and associated issues such as computational demand, are major constraints of mechanistic crop models especially when applied in a distributed setting to a large geographic domain, which necessitates a compromise between the level of complexity and the purpose of the modelling (Adam et al., 2011; Ramirez-Villegas et al., 2017).

Here, we employ a simplified agrohydrological modelling framework to assess the impacts of climate change on GWA and the subsequent effects on major cereal crops (teff, maize, sorghum, and wheat) produced in the entire RFA region of Ethiopia. We address three research questions that are relevant for future agricultural water management planning in Ethiopia: (i) what is the current green water availability and how will it change under the future climate across the RFA region?; (ii) how will these changes affect water-limited attainable crop yields (AY)?; and (iii) which hydroclimatic factor (rainfall or evapotranspiration) dominantly drives these changes and where? We base our assessment on crop response conditions where all crop growth factors except water are unlimited so that we can capture the effects of climate-driven changes in crop yields in a relative manner. Furthermore, we critically discuss the implications of the changes for water management in the NAP and similar agricultural development intiatives. We also present the workflow of our modeling framework to ensure its robust application in addressing similar or related agrohydrological research questions.

2. Methods

2.1. Study area

The study area covers the entire rainfed arable parts of Ethiopia (hereafter RFA region), as mapped in previous land use analysis (Kassawmar et al., 2018), encompassing an area of about 667,000 km^2 (59 % of the landmass of Ethiopia, see the blue outline in Figure 1a). The climate of the RFA region ranges from humid to semi-arid (Figure 1c) with mean annual potential evapotranspiration ranging from 700 mm in the highland regions to 1800 mm in the western lowland part of the RFA region. The mean annual rainfall of the RFA region ranges from 270 mm in the eastern part to 2100 mm in the western and

https://doi.org/10.5194/hess-2024-37
Preprint. Discussion started: 20 February 2024

Hydrology and Earth System Sciences
Discussions

95 southwestern parts (Figure 1b). The rainfall has unimodal patterns in the central, western, northern, and northeastern parts with highest rainfall in July/August depending on the location (Segele and Lamb, 2005; Wakjira et al., 2021). This rainy season typically spans from May to September, coinciding with the main growing season, locally known as 'Meher', during which approximately 88 % of the total annual crop harvest occurs (CSA, 2007). The southern and eastern parts of the RFA region on the other hand, largely experience a bimodal pattern with two rainy seasons in spring and autumn. The spring (February-May)
100 rainy period is considered the second and shorter growing season, locally known as 'Belg', in the southern and southeastern part of the RFA region. Cereals account for about 80 % of the crops produced, with teff, maize, sorghum, wheat, and barley being the top varieties, also serving as the main staple food crops in the country (CSA, 2007, 2010).

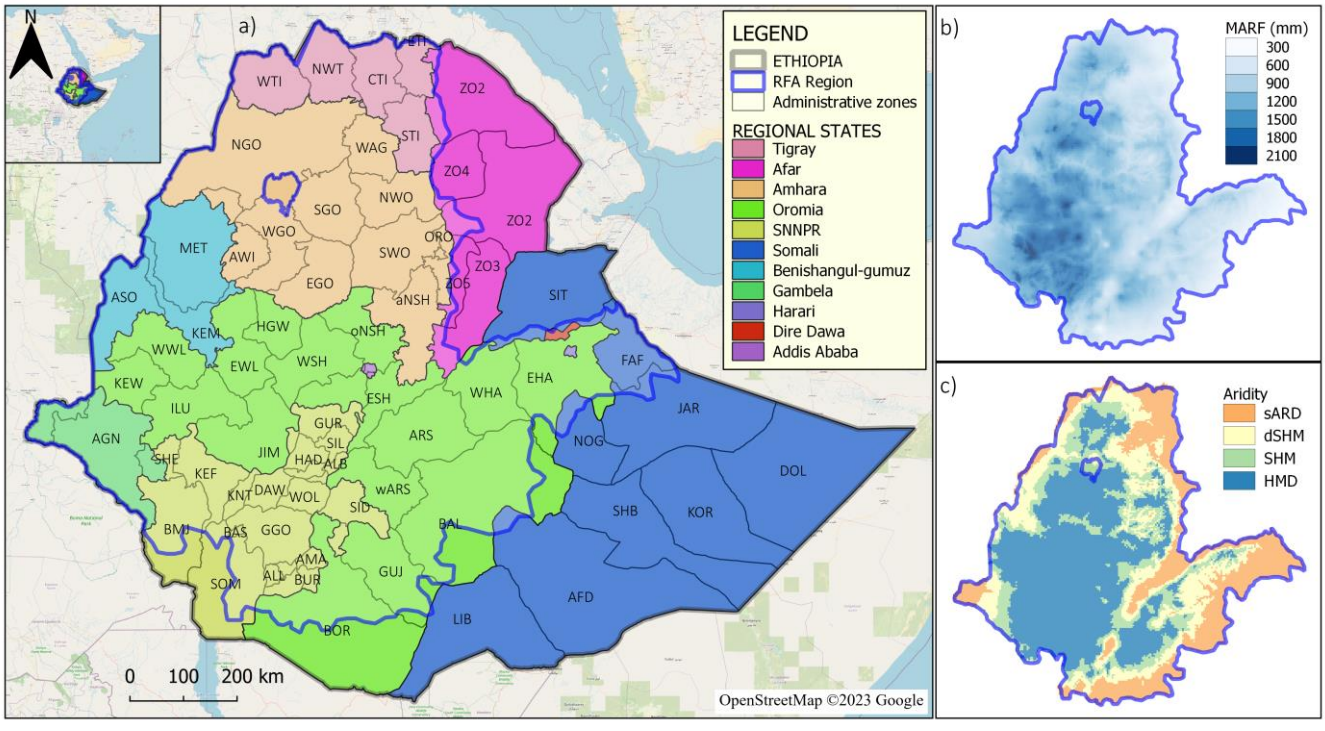

Figure 1: (a) Map of Ethiopia, the spatial extent of the rainfed agricultural region (blue outline, Kassawmar et al., 2018),
105 **administrative zones (designated by short names) in the nine regional states. The complete list of the zones with full names is given in Table S1. (b) Mean annual rainfall (MARF) of the RFA area for the period 1981-2010, based on CHIRPS. (c) Climatic regimes (aridity) of the RFA area (classification based on Spinoni et al. (2015)). sARD: semi-arid, dSHM: dry sub-humid, SHM: sub-humid, HMD: humid**

2.2. Data

110 Daily rainfall data for the reference period (1981-2010) was obtained from the Climate Hazards Infrared Precipitation with Station (CHIRPS) dataset (Funk et al., 2015), which is available at 0.05° x 0.05° spatial resolution. Maximum and minimum daily 2-m air temperature data consists of the bias-corrected and downscaled ERA5-Land (BCE5) dataset (Wakjira et al., 2022,

https://doi.org/10.5194/hess-2024-37
Preprint. Discussion started: 20 February 2024


Hydrology and Earth System Sciences
Discussions

2023), which is also available at 0.05° x 0.05° spatial resolution. Other climate variables (solar radiation, wind speed, and dew point temperature) were retrieved from ERA5-Land (Muñoz-Sabater et al., 2021) and disaggregated to a resolution of 0.05° x 0.05° using a bilinear interpolation method.

Future climate data were derived by downscaling multiple Global Circulation Model (GCM) projections, i.e., 26 for precipitation and solar radiation and 21 for maximum and minimum daily temperatures (listed in Table S2), from their native coarse resolution to 0.05° x 0.05° grid resolution using change factor (delta) approach (e.g., Anandhi et al., 2011; Teutschbein and Seibert, 2012). The future climate scenarios include three Shared Socioeconomic Pathways SSPs (Meinshausen et al., 2020; O'Neill et al., 2016), namely the SSP1-2.6 (low greenhouse gas emission), SSP2-4.5 (intermediate emission) and SSP5-8.5 (high emission).

Gridded soil texture and organic carbon content data were retrieved from SoilGrids (Poggio et al., 2021). Although the SoilGrids soil data is available at 250 m grid resolution, we upscaled the data to 0.05° (~5 km) to harmonize the spatial resolution with that of the climate datasets. Curve number (CN) values for agricultural land use were obtained from the USDA (1985) lookup table according to the hydrologic soil group dataset developed by Ross et al. (2018).

Independent actual evapotranspiration (ETa), surface runoff, and crop production datasets were utilized to evaluate the agrohydrological model simulations. ETa datasets were retrieved from five products – SSEBop (Senay et al., 2020), PML-v2 (Zhang et al., 2019), MOD16A2 (Mu et al., 2019), GLDAS 2.1 (Rui and Beaudoing, 2020), and TerraClimate (Abatzoglou et al., 2017), covering the period 2003-2010. Surface runoff data were collected from published runoff plot measurements at 17 locations (Table S3) across the RFA region of Ethiopia. Regarding the crop data, total cereal production (TCP), consisting of the sum of all cereals (maize, teff, sorghum, wheat, barley, millet, oat, and rice) produced in Ethiopia, was derived from the annual Agricultural Sample Survey (AgSS) reports (e.g., CSA, 2010) gridded by Wakjira et al. (2021) for the period 1995-2010.

2.3. Agrohydrological modelling

The agrohydrological modelling framework (Figure 2) that interlinks climate-hydrological-crop (CHC) interactions was developed to simulate the effects of climate change on green water fluxes, and its cascading influences on crop yield. The CHC model consists of three modules for climate, hydrology and crops.

https://doi.org/10.5194/hess-2024-37
Preprint. Discussion started: 20 February 2024

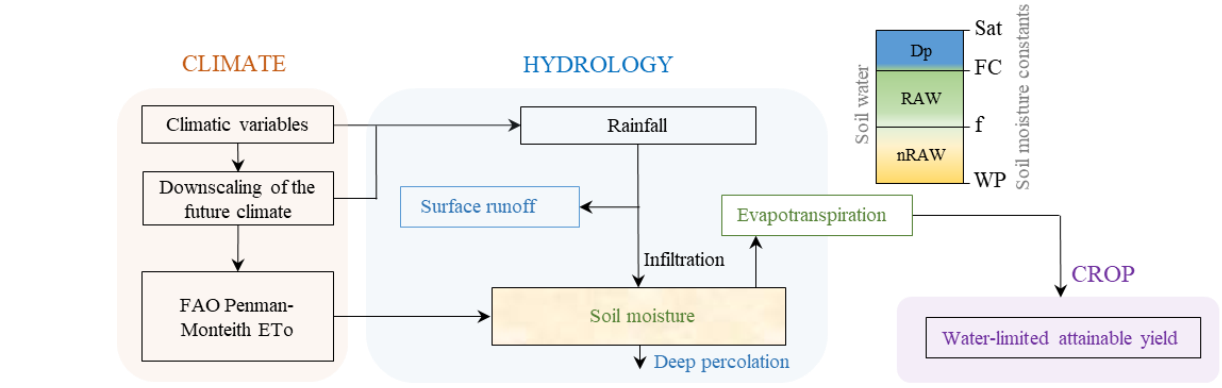

Figure 2: The CHC model used for the assessment of climate-driven changes in green water availability and water-limited attainable yields. Dp = deep percolation, RAW = readily available water, nRAW = non-readily available water, FC = field capacity, WP = wilting point, f = critical moisture depletion factor.

2.3.1. Climate module

The climate module uses climatic variables to compute the daily reference evapotranspiration ETo [mm d^{-1}] using the FAO Penman-Monteith equation (Allen et al., 1998):

$$\mathrm{ETo} = \frac{0.408\Delta(\mathrm{R_n}-\mathrm{G})+\gamma\frac{900}{\mathrm{T}+273}\mathrm{u_2}(\mathrm{e_s}-\mathrm{e_a})}{\Delta+\gamma(1+0.34\mathrm{u_2})}, \quad (1)$$

where R_n [MJ m^{-2}] is net radiation at the crop surface, G [MJ m^{-2}] is soil heat flux, T [°C] is 2-m mean daily air temperature, u_2 [m s^{-1}] is 2-m daily wind speed, $e_s - e_a$ [kPa] is saturation vapor pressure deficit, Δ [kPa °C^{-1}] is the slope of the vapor pressure curve, and γ [kPa °C^{-1}] is the psychometric constant.

2.3.2. Hydrology module

The hydrology module simulates the dynamic soil water balance without lateral surface and subsurface routing. A conceptual (bucket) water balance model is applied to the soil hydrological fluxes – surface runoff Q [mm], actual evapotranspiration ETa [mm], deep percolation Dp [mm], and changes in soil moisture ΔSM [mm] from rainfall input P [mm] at daily time step t:

$$\Delta\mathrm{SM_t} = \mathrm{P_t} - \mathrm{Q_t} - \mathrm{ETa_t} - \mathrm{Dp_t}. \quad (2)$$

Surface runoff is simulated according to the US Soil Conservation Service (SCS) curve number method (USDA, 1985):

$$\mathrm{Q_t} = \begin{cases} \frac{(\mathrm{P_t}-\mathrm{I_{a,t}})^2}{(\mathrm{P_t}-\mathrm{I_{a,t}})+\mathrm{S_{20,t}}}, & \text{if } \mathrm{P_t} > \mathrm{I_a} \\ 0, & \text{otherwise} \end{cases}. \quad (3)$$

https://doi.org/10.5194/hess-2024-37
Preprint. Discussion started: 20 February 2024


Hydrology and Earth System Sciences
Discussions

In the original SCS curve number model, the initial abstraction I_a [mm] was assumed to be 20 % of S (indicated by the subscript in Eq. (3)). However, recent insights led to an update in this value to 5 %, which yielded higher runoff prediction performance of the SCS model. A proposed conversion function from S_{20} to S_{05} is expressed by Hawkins et al. (2020):

$$S_{05} = 1.42 S_{20}. \quad (4)$$

S is determined by the land surface conditions including soil characteristics as represented by the hydrologic soil group, land use land cover (in our case agricultural land), and antecedent soil moisture, all of which are parameterized as a dimensionless CN value. We estimated S using Eq. (5).

$$S_{20} = 254\left(\frac{100}{CN} - 1\right). \quad (5)$$

CN is updated daily for antecedent moisture conditions (AMC), which are often categorized as *dry*, *normal*, and *wet*. The CN values obtained from the USDA lookup table correspond to the *normal* AMC condition. Accordingly, we estimated the CN values for the *dry* and *wet* AMC following Raes et al. (2022) and Smedema and Rycroft (1983):

$$\begin{aligned} CN_{dry} &= 16.91 + 1.348CN - 0.01379(CN)^2 + 0.0001172(CN)^3, \\ CN_{wet} &= 2.5838 + 1.944CN - 0.014216(CN)^2 + 0.000045829(CN)^3. \end{aligned} \quad (6)$$

We then adjusted CN at every time step by linearly interpolating between CN and CN_{dry} or CN_{wet} depending on the soil moisture condition, assuming the soil moisture content corresponds to θ_{WP} for CN_{dry}, $\theta_{0.5(\theta_{FC}+\theta_{WP})}$ for CN, and θ_{FC} for CN_{wet}.

Applying the conversion from Eq. (4) for S_{05} and then expressing I_a in terms of S_{20} in Eq. (3), the expression for Q can be rewritten as:

$$Q_t = \begin{cases} \frac{\left(P_t - 0.071 S_{20,t}\right)^2}{\left(P_t + 1.349 S_{20,t}\right)} & \text{, if } P_t > 0.071 S_{20} \\ 0 & \text{otherwise} \end{cases}. \quad (7)$$

The rainfall that is in excess of Q (Eq. (7)) infiltrates into the soil and refills the available soil storage V_t[mm] $= 1000Z(\theta_{sat} - \theta_{t-1})$, where θ_{sat} [m^3 m^{-3}] and θ_{t-1} [m^3 m^{-3}] are volumetric soil moisture content at saturation and on the previous day (respectively), and Z [m] is the soil depth. We considered that the top 60 cm homogeneous soil layer contains the majority of the root biomass (e.g., Fan et al., 2016; Mthandi et al., 2013), and hence this is the agrohydrological active soil depth Z for the major crops. ETa is determined by moisture availability (green water) relative to the readily available water, RAW [mm] $= 1000Zf(\theta_{FC} - \theta_{WP})$, where f [-] is a critical depletion fraction that represents the soil moisture level below

https://doi.org/10.5194/hess-2024-37
Preprint. Discussion started: 20 February 2024


Hydrology and Earth System Sciences
Discussions

which plants experience moisture stress. For all four cereal crops studied, the value of f was set to 0.55 following Allen et al. (1998). θ_{FC} [m^3 m^{-3}] and θ_{WP} [m^3 m^{-3}] are volumetric moisture contents at field capacity and wilting point and they were estimated using the widely used pedotransfer function developed by Saxton and Rawls (2006). ETa was computed as $ETa_t = K_{s,t}ET_{o,t}$, where *Ks* [-] is the soil moisture stress coefficient (Allen et al., 1998):

$$\mathrm{K_{s,t}} = \begin{cases} \frac{\mathrm{SM_t}}{\mathrm{RAW}} & \text{if } \mathrm{SM_t} < \mathrm{RAW} \\ 1 & \text{if } \mathrm{SM_t} > \mathrm{RAW} \end{cases}. \quad (8)$$

If the soil is saturated, the infiltrated water which is in excess of the soil field capacity percolates into deeper soil layers at the rate $Dp_t = 1000Z(\theta_t - \theta_{FC})$.

2.3.3. Crop module

The crop module simulates water-limited attainable yield (AY) based on the FAO water production function (Doorenbos and Kassam, 1979), which establishes a linear relationship between relative crop yield losses and seasonal crop water use under water-limited climatic conditions:

$$1 - \frac{\mathrm{Y_w}}{\mathrm{Y_p}} = \mathrm{K_y}\left(1 - \frac{\mathrm{ETa}}{\mathrm{ETo}}\right), \quad (9)$$

where Y_w [ton ha^{-1}] and Y_p [ton ha^{-1}] are water-limited and energy-limited potential yields (respectively), and K_y [-] is the yield response factor that accounts for the complex crop characteristics that determine the crop water use. We redefined for AY, the ratio of water-limited yield Y_w, and potential yield Y_p as a function of evaporative stress index $ESI = 1 - ETa/ETo$:

$$\mathrm{AY} = 100(1 - \mathrm{K_y ESI}). \quad (10)$$

The recommended K_y values were set to 1.25 for maize, 0.9 for sorghum, and 1.15 for wheat, obtained from the FAO irrigation and drainage paper 66 (Steduto et al., 2012), and to 1.04 for teff (Araya et al., 2011).

2.3.4. Model evaluation

The CHC modelling framework was not explicitely calibrated, all parameters were taken from literature and global dataset, however the results were validated with independent datasets. Due to the limited availability of observed data we could not conduct a formal validation, however we compared the simulated values against the two most important observed agrohydrological variables *Q* and ETa at annual scale. The simulated mean annual *Q* was compared to published mean annual runoff observations from 17 sites within the RFA region (Table S3). We used the Nash-Sutcliffe Efficiency (NSE, Nash and Sutcliffe, 1970) and coefficient of determination R^2 to quantify the prediction skill. Similarly, we compared the simulated annual cycle and seasonality of ETa with five independent satellite- and model-based ETa products for the period 2003-2010.

https://doi.org/10.5194/hess-2024-37
Preprint. Discussion started: 20 February 2024

Hydrology and Earth System Sciences
Discussions

Finally, we examined how temporal variations in AY explain variabilities in seasonal crop production. For this, we correlated AY and total cereal production (TCP) at each computation grid during the period 1995-2010.

2.4. Assessment of GWA and its yield potential

We evaluated the climatology of GWA and AY during the two growing seasons, Meher (May to September) and Belg (February to May) from the simulations for the reference period 1981-2010. We used soil moisture deficit (SMD) as a metric to evaluate GWA:

$$\mathrm{SMD} = 100\left(1 - \frac{\theta_{\mathrm{clim}}}{\theta_{\mathrm{FC}}}\right), \tag{11}$$

where θ_{clim} [m^3 m^{-3}] is the climatological mean seasonal soil moisture. *SMD* [%] is a dimensionless metric ranging from 0 (no moisture deficit) to 100% (maximum moisture deficit). The yield metric, *AY* [%], which was determined using Eq. (10) is also a relative quantity that explains the percentage of the energy-limited potential yield that can be viably attained under the actual water-limited conditions when all other agro-environmental factors such as nutrients are not limiting the yield, thus its values range from 0 (no yield) to 100% (potential yield). AY is nonlinearly related to SMD, decreasing with an increasing moisture deficit (Figure 3). This nonlinearity results from the combined effects of climatic and soil charateristics. Figure 3 also shows that attainable yield diminishes as the soil moisture deficit reaches its maximum, which is about 70% of the soil moisture at field capacity.

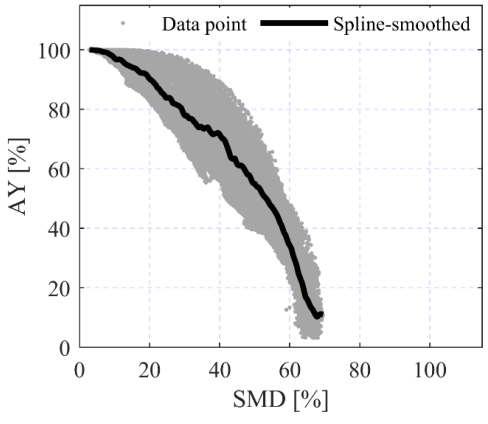

Figure 3: The relationship between AY and SMD in the RFA region of Ethiopia. Each data point represents a single grid cell in the RFA domain considering both Meher and Belg growing seasons.

2.5. Future changes and climate sensitivity analysis

We applied the modelling framework to quantify changes in GWA and its implications for AY under climate change. We investigated the changes for three future periods: 2020-2049 (2030s), 2045-2074 (2060s), and 2070-2099 (2080s), under SSP1-2.6 (low), SSP2-4.5 (intermediate), and SSP5-8.5 (high) greenhouse gas emission scenarios. The impact assessments presented

https://doi.org/10.5194/hess-2024-37
Preprint. Discussion started: 20 February 2024


Hydrology and Earth System Sciences
Discussions

here are based on the median of downscaled multiple GCM projections of future changes in rainfall, air temperature, and solar radiation. Other climatic variables were assumed to remain unchanged (Peleg et al., 2019). The impact analyses compare SMD and AY during the three future periods with the reference period (1981-2010) for the two growing seasons, Meher and Belg, and the four major crops grown in Ethiopia (teff, maize, sorghum, and wheat).

We also examined the sensitivity of AY to changes in rainfall (green water supply) and atmospheric evaporative demand (AED) as represented by ETo. We determined the rainfall- and AED-sensitivity metrics, $\beta_{RF} = \frac{\%\Delta AY_{(RF)}}{\%\Delta RF}$ [-] and $\beta_{ED} = \frac{\%\Delta AY_{(ED)}}{\%\Delta ETo}$ [-], as the ratio of percent change in *AY* and percent change in rainfall or *ETo* based on the one-at-a-time analysis approach (Hamby, 1994), where the CHC modelling framework was forced by the future RF and ETo (computed considering the future temperature and raditation) for all the three emission scenarios and three future periods. We determined the relative influences of the future changes in rainfall and AED on AY using the sensitivity ratio $\beta_{ratio} = \frac{\beta_{RF}}{\beta_{ED}}$. Values of β_{ratio} [-] range from zero to infinity with values less than one indicating temperature sensitivity dominates and values greater than one indicating AED sensitivity dominates. This assumes that changes in rainfall and ETo are independent, which was confirmed by the low dependency (R^2 = 0.098) between rainfall and *ETo* computed for the period 2020-2099 for the three SSPs at every grid point.

3. Results

3.1. Evaluation of the CHC model

We first evaluate the simulated runoff (*Q*), actual evapotranspiration (ETa), and water-limited attainable yield (AY) against other independent data. The comparison of simulated and observed mean annual *Q* (Figure 4a) at the 17 field locations demonstrates a good performance (R^2 = 0.80 and NSE = 0.53) of the hydrological module. It is important to note that this comparison involves a point-to-grid value, and a perfect match cannot be expected due to this scale difference. The model underestimates the simulated *Q* at the two most humid locations. The comparison for ETa was made for six arbitrarily defined sub-regions of the RFA region as shown in the inset in Figure 4b. The simulated mean annual ETa aligns well with the average estimates (hereafter, observed) from five independent ETa datasets (R^2 = 0.82), particularly in the north, northeast, and west sub-regions. Poorest fit is observed in the central sub-region where the model predicts higher ETa than observed, followed by the east sub-region where the simulated ETa is lower than observed. However, the simulated ETa estimates well the monthly cycles (Fig. S1) and annual ETa (Fig. S2).

We evaluated the simulations of *AY* [%] in terms of their correlation to variations in *TCP* [ton y^{-1}]. The rationale here is that in some regions TCP will follow the climate-driven attainable yield (high correlation), while in others the non-climatic factors, including nutrient input, improved cultivars, and pest and weed management, will play a role (low or negative correlation). Because TCP in the RFA region of Ethiopia exhibited an average increase of 0.36 ton ha^{-1} y^{-1} during the studied period (1995-2010), despite an almost constant AY, we conducted the correlation analysis on detrended TCP, thereby removing some of the

https://doi.org/10.5194/hess-2024-37
Preprint. Discussion started: 20 February 2024


Hydrology and Earth System Sciences
Discussions

effects of the non-climatic component of the variabilities in TCP (Kukal and Irmak, 2018; Mohammadi et al., 2023; Wakjira et al., 2021). The correlation analysis between detrended TCP and AY anomaly reveals mostly positive correlations (median Pearson's correlation coefficient, $\rho = 0.37$), particularly in the primary Meher-producing northern half of the RFA region (Figure 4c).

Some areas, primarily in the humid and sub-humid regions of the southern and southwestern parts, and to a lesser extent in the western and southeastern parts of the RFA region, exhibited negative correlations between TCP and AY. This can be attributed to climatic regimes, land use, and socioeconomic practices. Two main factors may govern the AY-TCP correlation with climate. In less water-limited humid areas like the southwestern part, the linear relationship assumed in the crop yield response to water availability (Eq.(9)) does not hold, as AY is weakly dependent on rainfall. Additionally, in these humid climates and areas with poor soil drainage (e.g., areas marked as E1 in Figure 4c), crop yield can be adversely affected by saturated soil conditions, leading to waterlogging problems. Concerning land use and socioeconomic practices, the majority of areas with evident negative correlation are forest and/or agroforestry ecoregions (see E2 and E3 in Figure 4c) (Kassawmar et al., 2018), while other areas are agropastoral (E4) where seasonal crop production is an optional practice. Thus, interannual variabilities in TCP depend largely on how much farmers opt for cereal production in a given production year.

https://doi.org/10.5194/hess-2024-37
Preprint. Discussion started: 20 February 2024

Hydrology and Earth System Sciences
Discussions

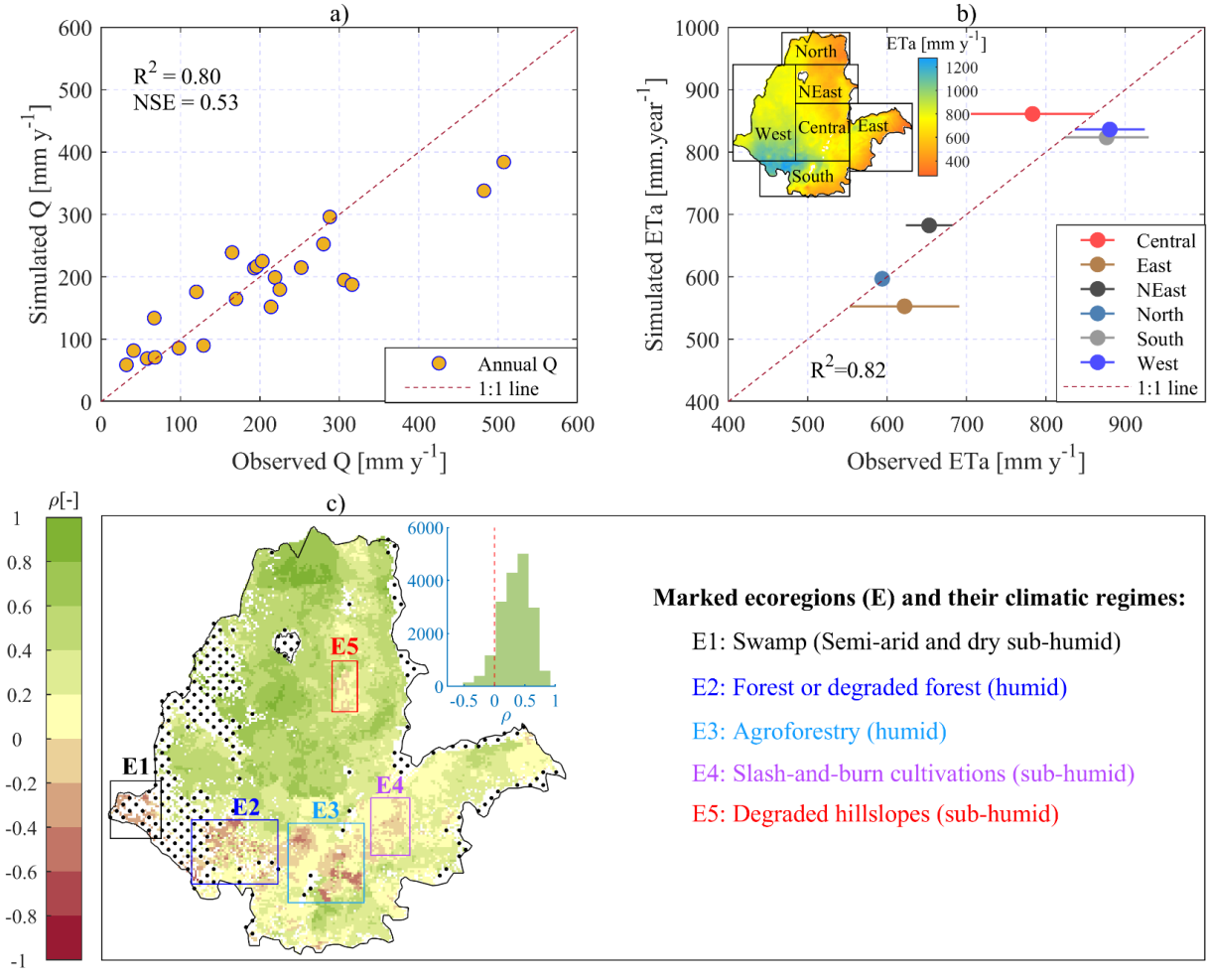

Figure 4: Comparison of: a) Simulated and observed yearly or mean annual runoff (Q), measured over varying years at 17 locations, collected from published studies across the RFA region (Table S3). This is a grid-to-point comparison. b) Simulated and satellite- and model-based mean annual ETa (2003-2010) from five data products (Sect. 2.2) spatially averaged over six arbitrarily defined sub-regions shown on the inset map. The error bars represent the variability (deviation from the median value) of ETa among the five products. c) Map of Pearson correlation coefficient (ρ) of detrended total cereal production (TCP) and AY for the period 1995-2010. TCP represents the sum of all cereals produced during the Meher growing season. The dots show uncultivated areas based on cropland cover fraction data from Copernicus Land Services (Buchhorn et al., 2020). The inset histogram shows the distribution of ρ. The rectangular marks (E1-E5) show ecoregions where the correlations are weak or negative.

https://doi.org/10.5194/hess-2024-37
Preprint. Discussion started: 20 February 2024


Hydrology and Earth System Sciences
Discussions

3.2. Green water availability and attainable crop yields

The reference climatology of growing season GWA and water-limited yield across the RFA region based on the computed SMD and AY values, is presented in Figure 5, considering alfalfa reference grass (Ky = 1.1). During the Meher growing season, the southern and southwestern humid regions of the RFA exhibit low soil moisture deficit, with values less than 10 % of θ_{FC} (see Figure 5a). Moving from the southwestern areas, the Meher SMD gradually increases in the northern and northeastern directions. In the peripheral semi-arid regions in the northeast, east, and southeast, the deficit reaches as high as 60-70 %. Notably, areas with SMD values below 20 % largely have AY>90 %. In other words, the water-limited yield gap less than 10 % of the potential yield achievable under unstressed moisture conditions (equivalent to fully irrigated system) can be attained in the south-central, southwestern, and eastern highland parts of the RFA region (Figure 5b). As expected, low AY (mostly less than 40 %) is evident in the southern and southeastern semi-arid parts of the RFA region during the Meher growing season. In summary, the median Meher SMD values are 17 %, 30 %, 37 %, and 53 % in humid, sub-humid, dry sub-humid, and semi-arid climates, respectively, while the corresponding median AY values are 93 %, 80 %, 68 % and 46 % (Figure 5e, f).

In the Belg season, the median SMD is mostly below 40 % in the major Belg-producing areas in the south (see Figure 5c), with AY of up to 80 % in the humid areas in the southwestern regions (Figure 5d). In the central and eastern parts of the RFA, which constitute other Belg regions, SMD is higher, reaching up to 60 %, resulting in a correspondingly lower AY of 40-60 %. The northern and northwestern parts of the RFA are dry during the Belg season, thus SMD is very high. Unlike in the Meher season, the differences in SMD among the climatic regimes are less pronounced, with median SMD ranging from 56 % in humid areas and 62 % in semi-arid regions (Figure 5e).

https://doi.org/10.5194/hess-2024-37
Preprint. Discussion started: 20 February 2024

Hydrology and Earth System Sciences
Discussions
Open Access
EGU

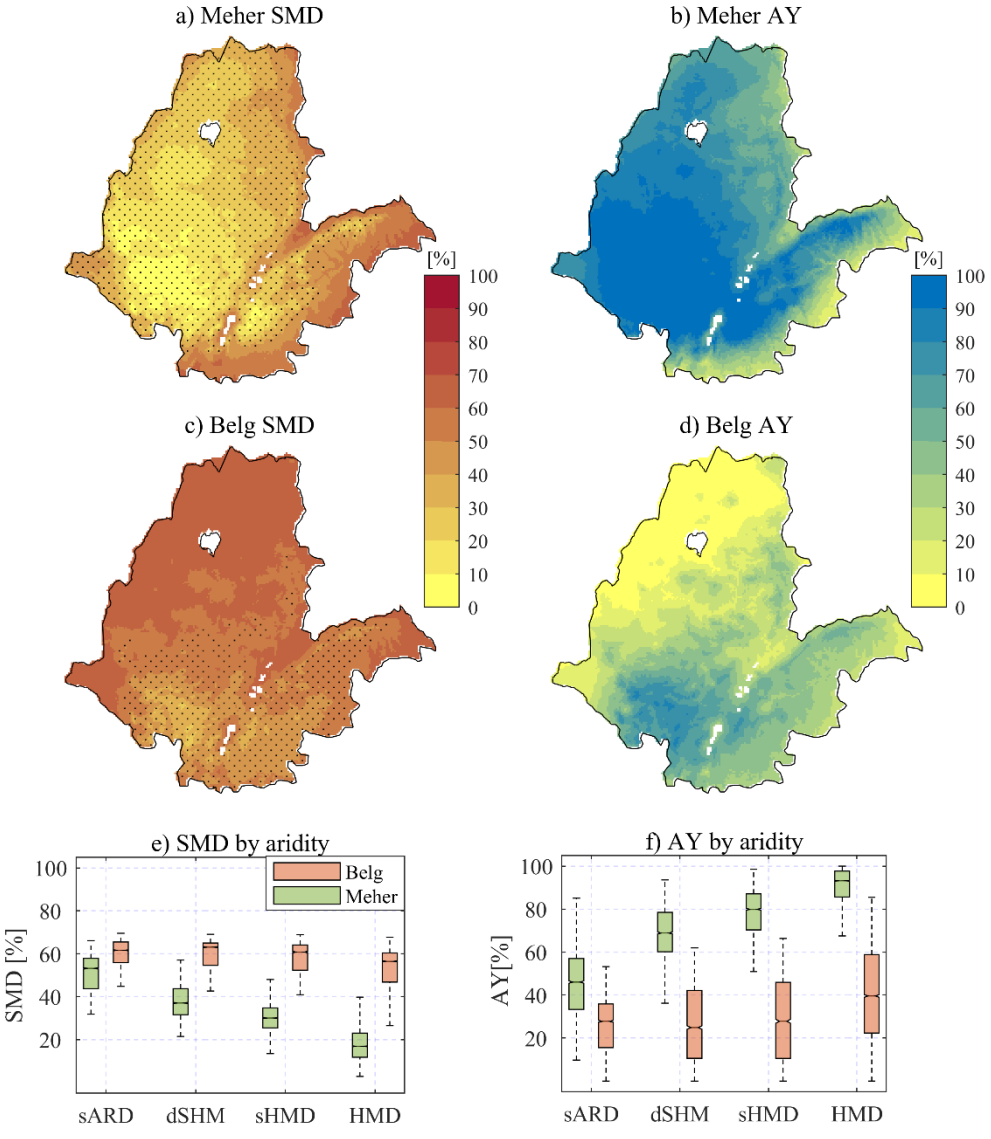

Figure 5: Climatological SMD during Meher (a) and Belg (c), AY for alfalfa grass (Ky = 1.1) during Meher (b) and Belg (d), SMD in different climatic regimes by aridity (e), AY in different climatic regimes during the two growing seasons for the period 1981-2010. Aridity classification is given in Figure 1: sARD = semi-arid, dSMD = dry sub-humid, sHMD = sub-humid, HMD = humid. The dotted areas in (a) and (c) show the Meher- and Belg-producing regions respectively, delineated based on the Atlas of Ethiopian Rural Socioeconomy (IFPRI and CSA, 2006).

https://doi.org/10.5194/hess-2024-37
Preprint. Discussion started: 20 February 2024

Hydrology and Earth System Sciences
Discussions

3.3. Future changes in GWA and AY

3.3.1. Projected changes in growing season rainfall and temperature

Based on the downscaled multiple GCM median projection, the growing season climate across the RFA regions is expected to become warmer and wetter in future periods (Figure 6). The temperature increase is progressive over time, especially under the intermediate and high emission scenarios, and shows little spatial variability (e.g., Figure 6c). However, changes in rainfall patterns vary across regions and depend on the growing seasons. For example, Meher-producing areas are likely to experience increased rainfall, while dry seasons are expected to remain unchanged or become even drier (e.g., Figure 6a, b). Similarly, during the Belg season, the Belg-producing areas in the southern part of the RFA region are expected to become wetter under higher greenhouse gas emissions. In general, a rainfall increase of up to 250 mm is anticipated over a large part of the RFA region during the Meher season under the high emission scenario in the 2060s (Figure 6a) and up to 300 mm in the 2080s (not shown). During the Belg season, rainfall changes could reach up to 150 mm under the high emission scenario in the 2060s. Additionally, the mean annual temperature is projected to rise by up to 3 °C in the 2060s and up to 5 °C by the end of the century.

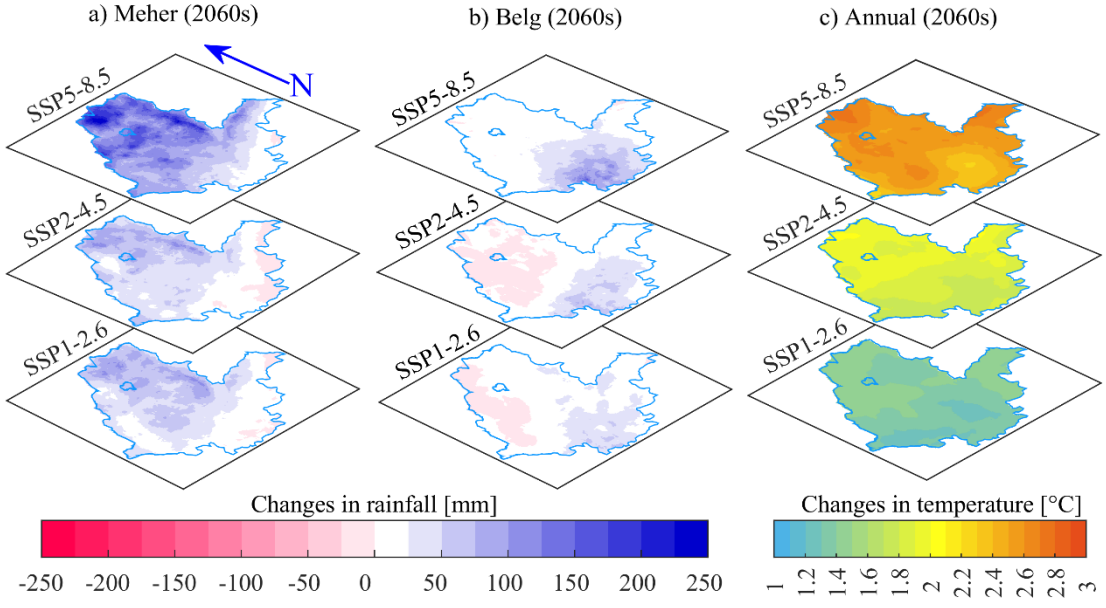

Figure 6: Projected changes in seasonal rainfall in the 2060s during a) Meher (May-September), b) Belg (February-May), and c) changes in annual temperature under the three SSPs. The changes presented here are the median of 26 downscaled GCM projections for rainfall and 21 GCM projections for temperature.

https://doi.org/10.5194/hess-2024-37
Preprint. Discussion started: 20 February 2024

Hydrology and Earth System Sciences
Discussions

3.3.2. Future changes in soil moisture deficit

In the face of the expected warmer and mostly wetter climate across the RFA region of Ethiopia, the GWA is likely to increase. In the main growing season, Meher, SMD is expected to decrease by up to 5 % over a large part of the region in the 2030s under all emission scenarios (Figure 7). However, in the 2060s and 2080s, SMD is projected to increase by 3-15 % over the western, southwestern, and southern parts under the low and intermediate emission scenarios. Under the high emission scenario, soil moisture deficit is likely to decrease over the majority of the region, following the increase in rainfall. The central and northeastern parts of the RFA regions are generally expected to experience a slight decrease in SMD and thus slightly higher GWA under all scenarios in the future. The highest increase in SMD was observed in the southwestern and southern parts of the RFA region, where the Meher rainfall mostly remains unchanged (see Figure 6a).

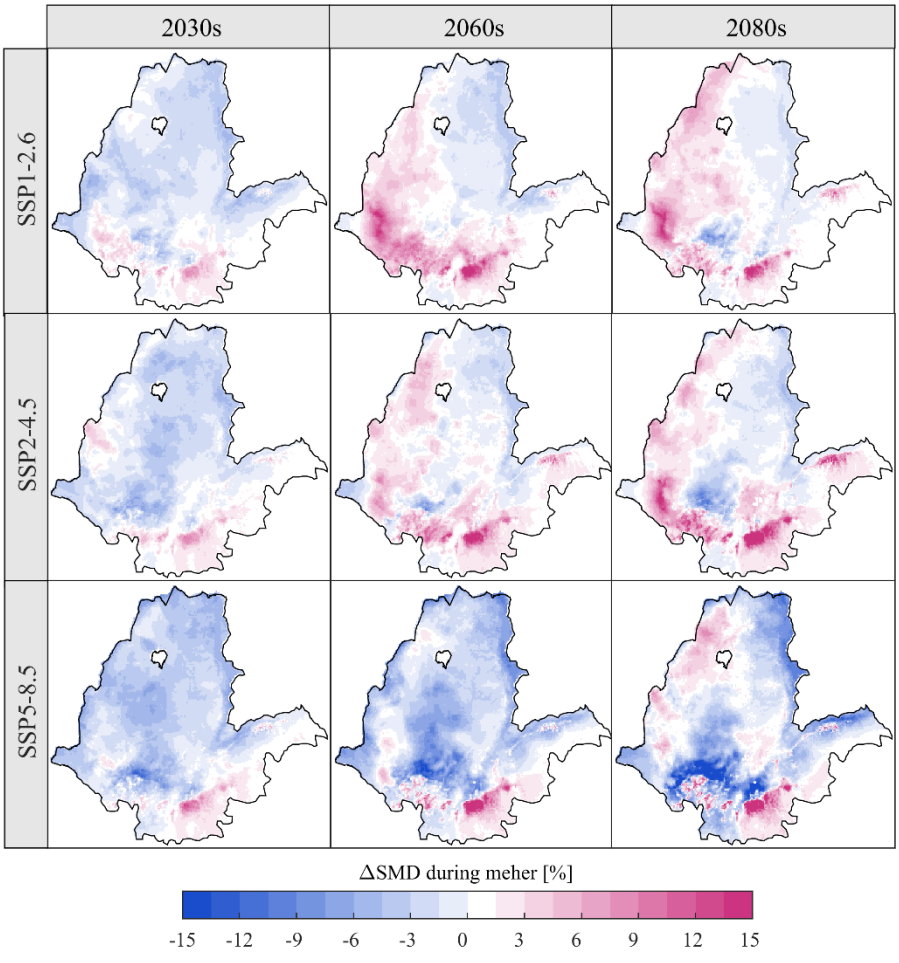

Figure 7: Projected changes in soil moisture deficit (SMD) across the rainfed agricultural region of Ethiopia during the Meher growing season under the SSP1-2.6, SSP2-4.5, and SSP5-8.5 in the 2030s, 2060s, and 2080s.

https://doi.org/10.5194/hess-2024-37
Preprint. Discussion started: 20 February 2024

Hydrology and Earth System Sciences
Discussions

In the Belg growing season, soil moisture deficit consistently decreases over the producing regions in the future periods under all scenarios (Figure 8). These increases in GWA are particularly significant across the main Belg region in the southwestern parts of the RFA. In these areas, SMD is expected to decrease by up to 6 % in the 2030s (2020-2049) and by over 15 % in the 2080s under the low and intermediate emission scenarios. Under the high emission scenario, GWA across the primary Belg-producing regions in the south and southwest is expected to increase by up to 35 % by the end of the century. Overall, the projected changes in soil moisture deficit across the study area are largely consistent with a recent global-scale assessment by Liu et al. (2022), which reported a decrease in agricultural water scarcity of up to 15 % in the RFA region for a comparable future period (2026-2050) and reference period (1981-2005) under the RCP2.6 scenario.

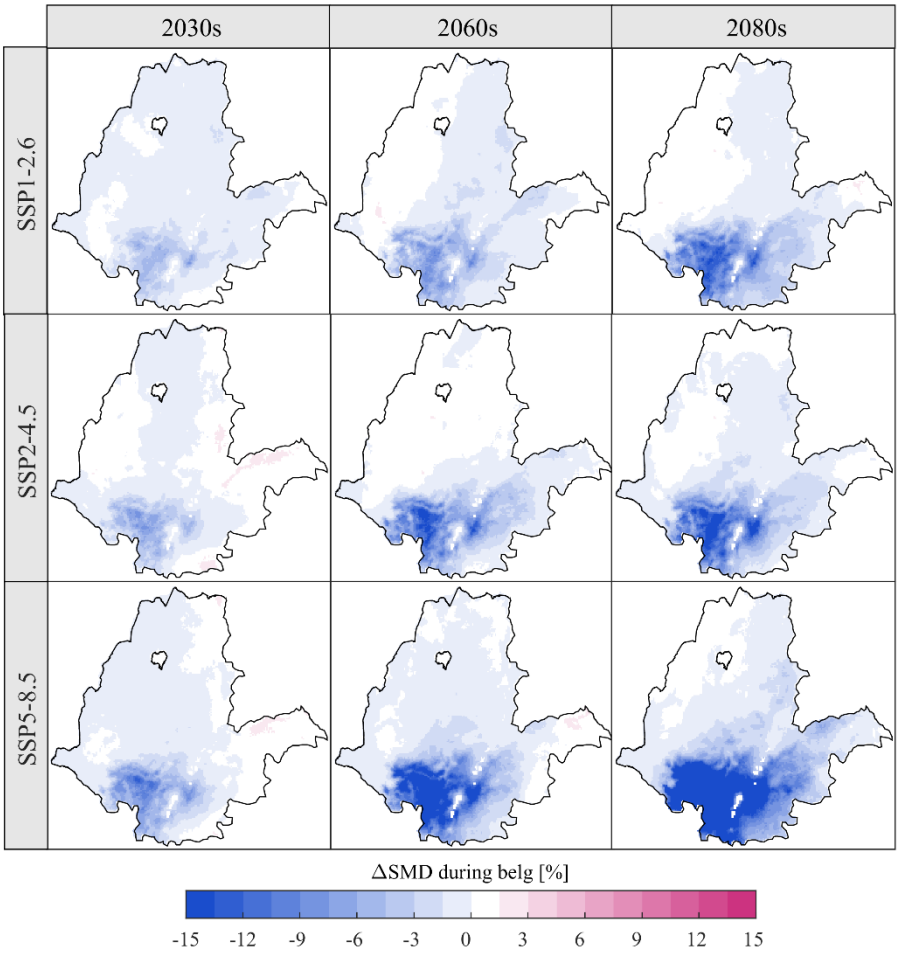

Figure 8: The same as Figure 7 but for the Belg growing season

3.3.3. Future changes in water-limited crop yields

https://doi.org/10.5194/hess-2024-37
Preprint. Discussion started: 20 February 2024


Hydrology and Earth System Sciences
Discussions

The likely implications of changes in SMD on attainable yields for the four major cereal crops (teff, maize, sorghum, wheat) cultivated in Ethiopia are presented next. We summarize the changes occurring during the two growing seasons in their respective producing regions and across the various climatic regimes of the RFA.

https://doi.org/10.5194/hess-2024-37
Preprint. Discussion started: 20 February 2024

Hydrology and Earth System Sciences
Discussions
Open Access
EGU

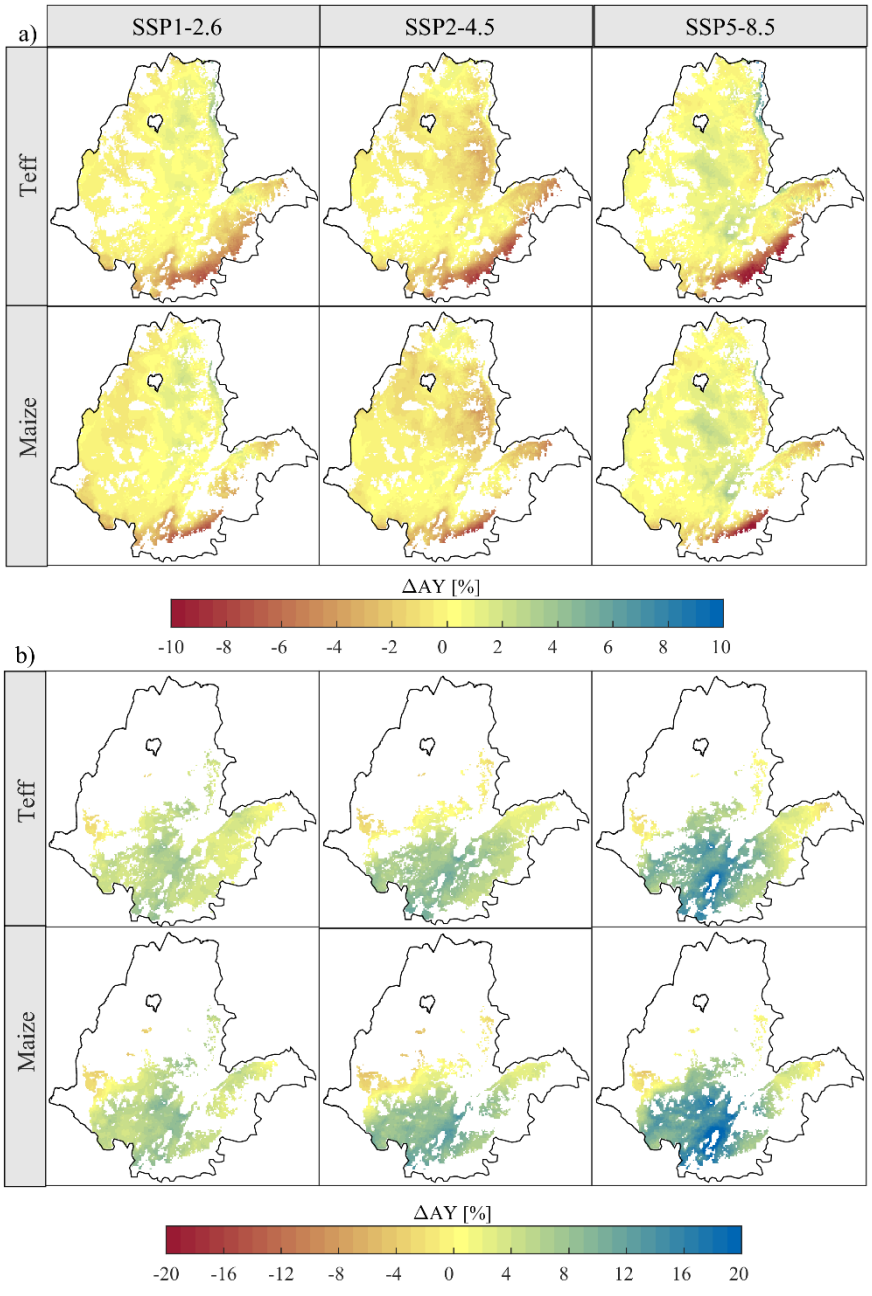

Figure 9: Projected changes in water-limited attainable yield for teff and maize in Meher (a) and Belg (b) during the 2060s under the SSP1-2.6, SSP2-4.5, and SSP5-8.5. The RFA region was masked using cropland suitability maps (Wakjira et al., under review) to restrict the analysis to areas potentially suitable for each crop. The non-producing areas during both seasons were also masked out following the Atlas of Ethiopian Rural Socioeconomy (IFPRI and CSA, 2006).

https://doi.org/10.5194/hess-2024-37
Preprint. Discussion started: 20 February 2024


Hydrology and Earth System Sciences
Discussions

Meher season

In the Meher season, minor or no changes in AY are expected, although regional differences exist in both the magnitude and direction of these changes. For example, during the 2060s, the projected changes in AY for teff range from -7.8 % to 5.3 % under the low-emission scenario, and from -12.1 % to 10.7% under the high-emission scenario. Similarly, for maize, the expected changes range from -7.8 % to 4.7 % under the low emission scenario, and from -11.5 % to 6 % under the high emission scenario (Figure 9a). Under the intermediate emission scenario, the changes are predominantly negative, ranging from -9.3 % to 1.8 % for teff and from -8.2 % to 1.2 % for maize. Similar order of magnitude and direction of changes were observed for sorghum and wheat crops (refer to Fig. S3-7).

Comparing the near- and long-term future changes, we note a decreasing trend in AY for all crops under all emission scenarios. During the 2030s, the northern parts of the RFA region are likely to experience increases, while decreases are mainly evident in the southern and southeastern parts of the Meher-producing areas. Notably, the marginal areas in the south and southeast are likely to experience the most significant decrease in AY for all crops and under all scenarios. By the 2080s, most Meher-producing areas are expected to witness either no change or a decrease in AY (Fig. S3-7).

We also examined the water-limited attainable yield responses in different climatic regimes (Figure 10). In humid areas, the temporal changes and spatial variability in AY are small for all crops under all emission scenarios. This is because these areas rarely have moisture limitations, meaning that an increase in rainfall will have a minimal effect on yield improvement. In contrast, in semi-arid, dry sub-humid, and sub-humid areas, AY is likely to increase in the 2030s and then consistently decrease in future periods under both low and high emission scenarios. Under the intermediate scenario, AY is expected to decrease in the 2060s and then increase in the 2080s. Spatial variations are particularly high for teff, especially in semi-arid areas with changes ranging from -10 % to +5 % in the 2060s.

Belg season

Following the increased rainfall and the subsequent rise in GWA, AY is projected to increase significantly and progressively over the major parts of the Belg-producing regions in future periods. However, a few areas will experience small decreases (Figure 9b). For teff, the expected changes in the 2060s range from -3.5 % to 8.8 % under the low emission scenario and from -3.6 % to 21.7 % under the high emission scenario. Similarly, for maize, the changes range from -5.9 % to 10.6 % under the low-emission scenario and from -4.7 % to 27.6 % under the high-emission scenario. These positive changes are expected to intensify, particularly under the high emission scenario, with the majority of the Belg-producing region experiencing an increase in AY of over 20 % for all crops examined. The changes for all crops and future periods have been illustrated in the supplementary material appended to this paper (Fig. S7-10).

https://doi.org/10.5194/hess-2024-37
Preprint. Discussion started: 20 February 2024

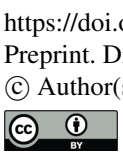

Hydrology and Earth System Sciences
Discussions

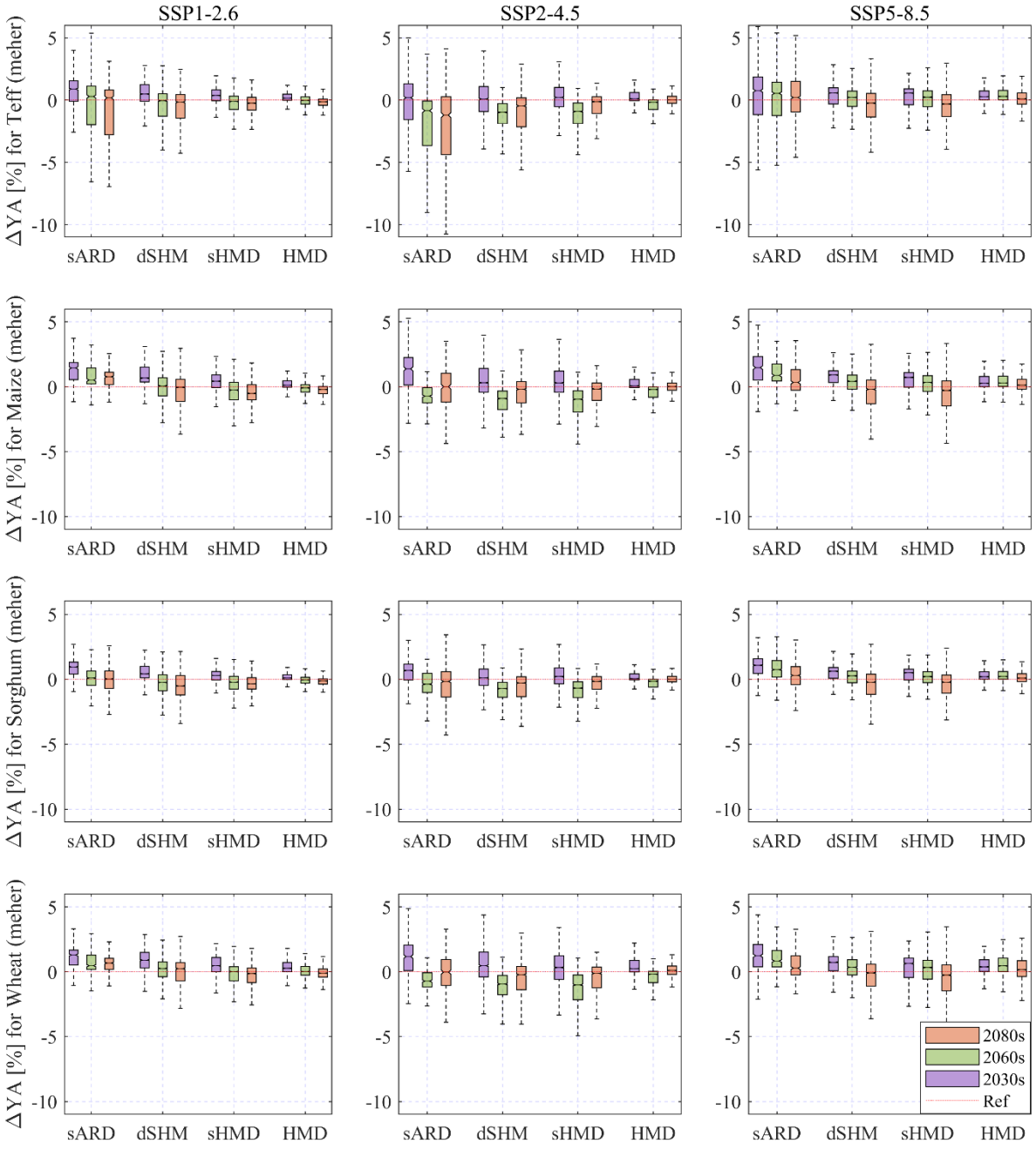

380

Figure 10: Boxplots of the projected changes in water-limited yields (AY) of the four major cereal crops produced in Ethiopia in different climatic regimes under the three SSPs during the three future periods, during the Meher growing season. Each boxplot represents the distribution of AY changes within Meher-producing areas for all grid cells in the respective climatic regime. Outlier values have been excluded.

https://doi.org/10.5194/hess-2024-37
Preprint. Discussion started: 20 February 2024


Hydrology and Earth System Sciences
Discussions

385

The changes in AY during the Belg season in different climatic regimes are illustrated in Fig. S11. The variations in overall changes in AY among these regimes depend on the emission scenario. Under the low emission scenario, median changes in AY do not significantly vary across climatic regimes, remaining positive throughout the three future periods for all crops
390 examined. In contrast, under the intermediate and high emissions, AY tends to increase with climatic wetness (from semi-arid to humid climates).

Decreases in AY are mainly noticeable in semi-arid and dry sub-humid areas in the 2030s. However, during the 2060s and 2080s, median changes in AY are relatively consistent across climatic regimes for all crops. Spatial variability in changes generally increases with climatic wetness and into the future periods under the low emission scenario while a decreasing pattern
395 rarely observed under the intermediate and high emission scenarios. In all cases, spatial variability of the changes is lower in the 2030s compared to the mid- and long-term future periods. Concerning the examined crops, it was observed that the projected increases in AY are higher for maize and wheat compared to teff and sorghum.

3.3.4. Climate sensitivity of attainable crop yields

The spatiotemporal average relative sensitivity (β_{ratio}) of AY to atmospheric evaporative demand (AED) and rainfall for the
400 four crops under the three SSPs are presented in Figure 11. The results are averaged for the three future periods for the main growing season Meher at the administrative agricultural zones of Ethiopia. Results for the Belg short growing season are presented in Fig. S12. The climate sensitivity is reported at a zonal scale, rather than at the grid scale, to provide zone-specific insights into the relative importance of ETo and rainfall that determines future green water supply; this information is crucial for agricultural water management planning, service provision, and decision-making at the institutional scale. For the
405 interpretation, we categorize the sensitivity of AY as AED-sensitive ($\beta_{ratio} \leq 0.8$), AED- and rainfall-sensitive ($0.8 < \beta_{ratio} < 1.2$), and rainfall-sensitive ($\beta_{ratio} \geq 1.2$).

During the Meher growing season, AY is predominantly AED-sensitive for all crops under all emission scenarios we considered (Figure 11). The percentage of zones across which AY is, on average, AED-sensitive is 64 % for teff, 50 % for maize, 52 % for sorghum and 77 % for wheat under low emissions. The influences of AED on AY increase with GHG
410 emissions. Under high emissions, AED dominates the changes in AY in 82 %, 65 %, 73 %, and 92 % of the zones for teff, maize, sorghum, and wheat respectively. In the remaining zones, the simultaneous influences of rainfall and AED are evident, except for maize, where rainfall has a more significant impact than AED. Notably, changes in rainfall have a low influence on teff and wheat, with AY being rainfall-sensitive in less than 5 % of the zones. These crops are exceptionally more sensitive to AED compared to maize and sorghum, as indicated earlier. Temporal changes in climate sensitivity of AY are also evident,
415 but the spatial patterns do not change significantly in future periods.

https://doi.org/10.5194/hess-2024-37
Preprint. Discussion started: 20 February 2024


Hydrology and Earth System Sciences
Discussions

The influences of changes in AED and rainfall on AY are primarily linked to the climatic regimes of the RFA region. In semi-arid and dry sub-humid climates, AY is predominantly AED-sensitive. This is particularly noticeable in the northeastern zones (covering the eastern parts of Tigray and Amhara, and western zones of Afar regions) and the central to eastern zones (including East Shoa, Arsi, and Hararge zones of the Oromia region) in the RFA region for all crops under low emissions (left panels in Figure 11). The influence of AED intensifies to more zones in sub-humid and humid climates under the intermediate and high emissions. Rainfall-sensitivity is largely evident in humid climates, mostly in the central, western, and northwestern zones under low emissions for all crops except wheat, which is rainfall-sensitive only in the northwestern parts of the RFA region (Western Tigray and North Gonder zones). Maize AY is strongly rainfall-sensitive under all scenarios, across the humid zones in the western part of Oromia (Wollega, Jimma, and Illubabor zones), Sidama region, and most of the zones of the SNNP region in the southwestern part. AED-sensitivity intensifies to cover more zones in sub-humid and humid climates under intermediate and high emissions.

In contrast to the main growing season, future changes in AY during the Belg growing season are primarily influenced by changes in rainfall, particularly in the main Belg-producing areas in the southwestern, southern, and southeastern parts of the RFA region for all crops under all SSPs (Fig. S12). There is less spatio-temporal change in the rainfall sensitivity of Belg AY. Only under the high emission scenario does the influence of changes in AED contribute to the influences of rainfall, primarily in the northern half of the RFA region, which remains dry during this season.

https://doi.org/10.5194/hess-2024-37
Preprint. Discussion started: 20 February 2024

Hydrology and Earth System Sciences
Discussions

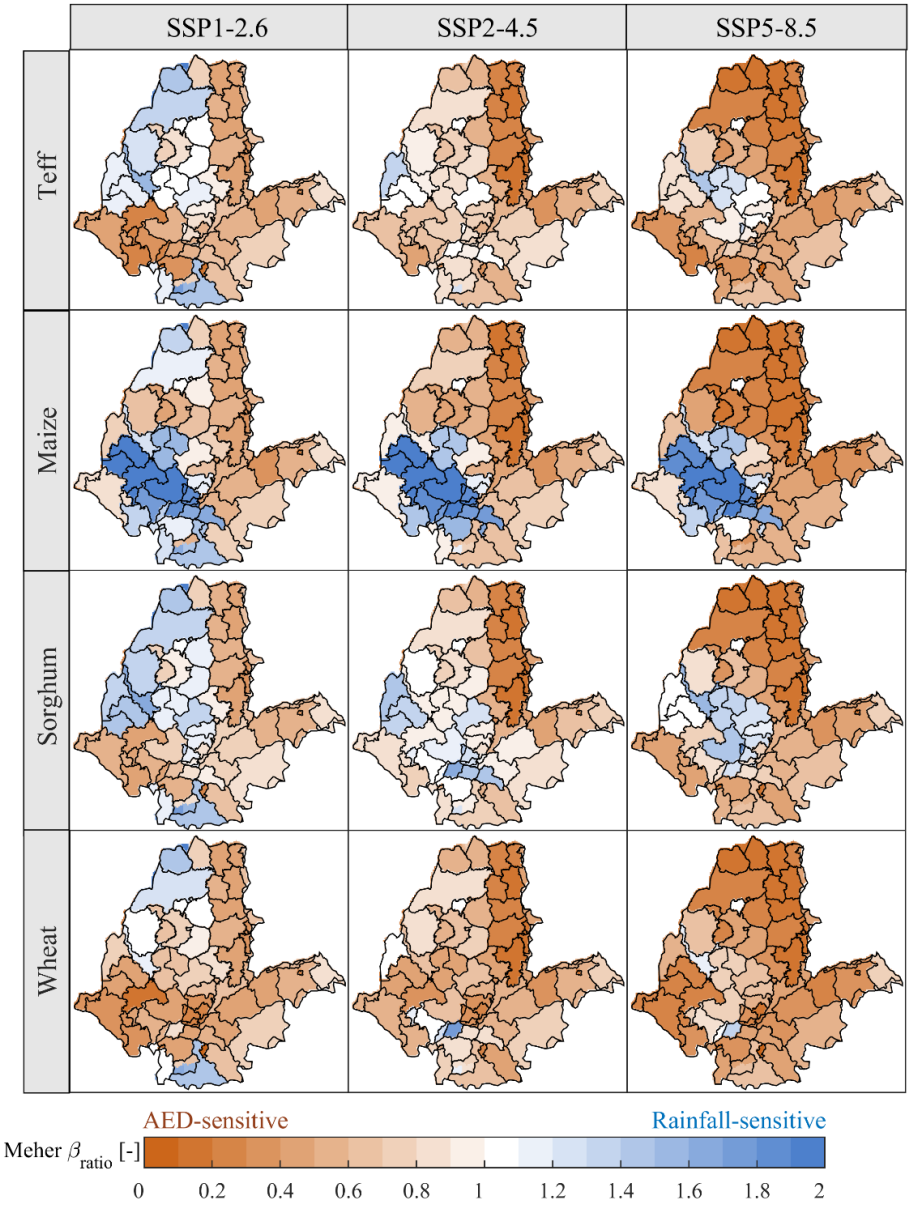

Figure 11: Area-averaged relative sensitivity (β_{ratio}) of water-limited attainable yields (AY) to rainfall and atmospheric evaporative demand (AED) for the Meher growing season at the administrative zone level under the low, intermediate, and high emission scenarios. The mapped values represent the average of β_{ratio} of all grid cells within each zone, and all three future periods. The names of the administrative zones are indicated in Figure 1 and Table S1.

https://doi.org/10.5194/hess-2024-37
Preprint. Discussion started: 20 February 2024


Hydrology and Earth System Sciences
Discussions

4. Discussion

4.1. Current water limitations and crop yield gaps

Achieving crop yield at its potential level is not only a matter of adaptation to climate variability and change, but it is also a key strategy for eradicating rural poverty and building resilience in heavily agricultural nations like Ethiopia (Abrams, 2018; Tittonell and Giller, 2013). In the effort to enhance crop yields, three levels of yields can be defined and targeted (van Ittersum et al., 2013): (i) potential yield (Yp), primarily defined by temperature, radiation, light, and cultivar; (ii) water-limited yield (Yw), determined by moisture availability and soil type, but within the constraints of Yp; and (iii) actual yield (Ya), which is dependent mainly on farm management practices including water, soil, nutrient, pest and weed management. In RFA systems water is a major limiting factor, and thus, Yw defines the rainfed crop yield potential (Dijk et al., 2017; van Ittersum et al., 2013), as Yp can be reached only by supplementing the green water through irrigation to fully meet the crop water demand.

Figure 12 illustrates the current conditions of the three yield levels in a Budyko-like space (Budyko, 1958) and analyzes the yield gaps with AY. In the Meher season, green water has the potential to produce more than 80 % of Yp across 52 % of the Meher-producing regions of Ethiopia (highlighted by the shaded area in Figure 12a). Only about 27 % of the Meher-producing region is moisture-limited (P/ETo < 1). However, there are areas where the seasonal rainfall is greater than the atmospheric evaporative demand, but AY is still low (e.g., shown by the red ellipse in Figure 12a). This discrepancy is primarily linked to surface and soil characteristics that influence rainfall-runoff partitioning and green water storage capacity. From a management perspective, there may be limited options to address inherent soil physical properties like textural composition, apart from measures such as amendment with organic matter, which might to some extent, improve infiltration and green water storage capacity (Hartmann and Six, 2023).

On the other hand, there is an extremely large yield gap between Ya (orange rectangle symbols) and Yw (blue diamond symbols) as shown in Figure 12a, for maize for example. Our comparison of Yw from data reported at 14 experimental case studies across the RFA region (see Table S3), and the corresponding zone-averaged Ya from the agricultural sample survey of Ethiopia (e.g., CSA, 2010) shows that the absolute yield gap at these sites ranges from 1.3 to 7 ton ha^{-1} (Figure 12b). This gap should be reduced by addressing farm management actions, including tillage, resources use (green water and nutrient management, cultivar selection) and crop protection (pest and weed management) (Lobell et al., 2009). Other limitations like soil salinity, acidity, and waterlogging are also among the yield-reducing factors that need a substantial amount of financial and technological investment.. Our previous work has shown that actual crop yields are also greatly influenced by seasonal rainfall characteristics such as timing (onset and cessation) and seasonal distribution (Wakjira et al., 2021), which suggests that measures like onset-informed planting (Lala et al., 2021) could be beneficial to reduce the yield gaps associated with water stress in moisture limited areas.

https://doi.org/10.5194/hess-2024-37
Preprint. Discussion started: 20 February 2024

Hydrology and Earth System Sciences
Discussions
Open Access
EGU

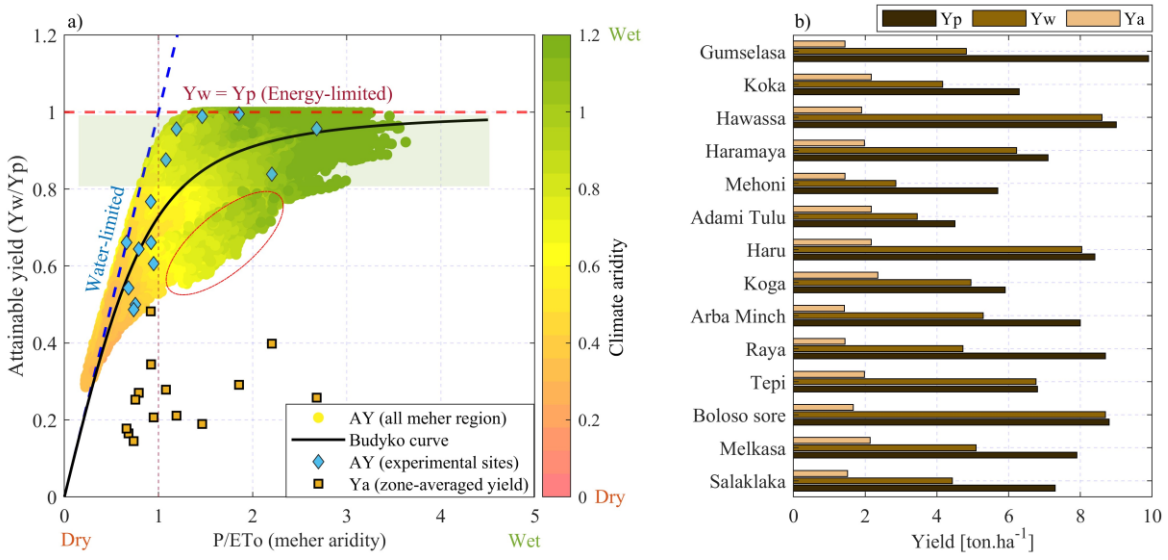

Figure 12: a) Scatterplot of water-limited attainable maize yield fraction (Yw/Yp) against seasonal aridity showing the energy (dashed red line) and water limitations (dashed blue line). The color gradient shows the climatic aridity of each grid cell (different from the values on the x-axis, which are seasonal aridity). The solid line represents the parametric Budyko curve fitted to the point cloud. The blue diamonds show Yw at 14 locations across the RFA region, derived from published maize Yp data (fully irrigated, optimally fertilized). The orange squares are the corresponding average actual maize yield (Ya) in the administrative zone within which the experimental location is found. The shaded area indicates maize AY>80 %. b) Comparison of Yp (experimental), Yw (derived as a fraction of Yp using AY), and Ya (also as a fraction of Yp). The list of experimental locations is given in Table S3.

4.2. Implications for agricultural water management

While the changes in water-limited attainable yield vary greatly across the RFA in terms of both magnitude and direction during the main growing season, the results show that semi-arid and dry sub-humid areas are most likely to experience a reduction in AY. On one hand, this is attributed to an intensified soil moisture deficit, as evident for example in the northwestern, western, southern, and southeastern semi-arid areas (with low and intermediate emissions in the 2060s and 2080s, in Figure 7), and on the other hand, it is also a result of increases in AED-sensitivity (Figure 11), particularly in the moisture-limited regions. In these regions it would be beneficial to implementat on-farm water management strategies that maximize green water availability and minimize non-productive green water flows.

Practices that aim to maximize GWA should focus on altering the rainfall-runoff partitioning processes by increasing the opportunity for infiltration during rainfall through various surface management practices. For example, tillage and physical measures like bunds, infiltration trenches, tied-ridge, and planting pits among others (Hurni, 2016; Makurira et al., 2009; Nyakudya et al., 2014) have been successfully evaluated in field experiments and on-farm practices. Other measures like residue retention and cover cropping not only enhance infiltration, but also suppress the non-productive evaporation from the

https://doi.org/10.5194/hess-2024-37
Preprint. Discussion started: 20 February 2024


Hydrology and Earth System Sciences
Discussions

soil surface. (Rockström, 2003). Additionally, measures that improve infiltration also offer the side benefit of reducing soil erosion by runoff, another critical challenge that contributes to the crop yield gap. Finally, we strongly suggest that the selection of water management practices should be carefully made by evaluating their need and suitability primarily based on climate and soil characteristics. For example, in humid climates with heavy clay soils, such practices may result in waterlogging problems, which is also a major yield-reducing factor in such environments (Manik et al., 2019; Pittelkow et al., 2015).

4.3. Intensification of the Belg season production

The projected increase in GWA and AY during the Belg season may provide an additional opportunity for farmers to intensify their production during this season. This, however, will need firm stakeholder commitment to plan and mobilize resources for action in the framework of National Adaptation Plans (NAP) and similar initiatives (Conway and Vincent, 2021). Long-term awareness of stakeholders, ranging from the institutional level to farm-level actors, on the expected challenges and opportunities of climate change, supported by climate information services for short-term decisions, is highly important to exploit such opportunities (Grossi and Dinku, 2022). In addition to climate information like the forecast information of the expected onset and cessation of Belg rain, extensive support on proper selection of crop types compatible with the duration of the short growing season is vital to help farmers effectively plan and undertake bi-annual production without compromising the main growing season. Moreover, the high soil moisture deficit (Figure 5) and high sensitivity of water-limited yield to rainfall during this season (Fig. S12) suggest that green water management practices are crucial for enhancing productivity.

5. Conclusions

We investigated the cascading effects of climate on green water availability and water-limited attainable yield (AY) in the context of the rainfed agricultural region of Ethiopia. We integrated hydroclimatic processes with crop yield response through an agrohydrological modelling framework to assess the current potential, future changes, and climate sensitivity of AY. The AY across the Ethiopian RFA region is 79 % of what could be produced under water-unlimited conditions during the main growing season (Meher) and 37 % during the shorter season (Belg) during the reference period, with regional variation depending on the climatic regimes. The soil moisture deficit (percent of soil moisture content at FC) during this period is on average about 29 % in Meher and 56 % in Belg.

The future climate over the RFA region is expected to be warmer and mostly wetter. Under these changes, future changes in green water availability and AY vary across regions, emission scenarios, future periods, and between the two growing seasons. In Meher, the expected changes in AY range largely in the ±5 % range under all scenarios and future periods. Changes during the 2030s are largely positive under all scenarios, but AY shows overall decreases in the 2060s and 2080s. Decreases in AY are mostly evident in semi-arid regions, with teff being the most affected. These changes are dominantly driven by the atmospheric evaporative demand (AED), that is by temperature increase, especially in moisture-limited regions. The influence of AED increases under the intermediate and high emission scenarios, suggesting the need for due attention to management strategies that suppress evaporative losses in the future. In Belg, AY is expected to progressively increase by up to 20 % under

https://doi.org/10.5194/hess-2024-37
Preprint. Discussion started: 20 February 2024


Hydrology and Earth System Sciences Discussions

the high emission scenario by the end of the century, providing an opportunity for farmers to expand crop production in this season. These changes are dominantly driven by increases in rainfall, implying that green water management practices that increase water availability would further improve crop yields during this season. Furthermore, our assessment of documented field experiment results and crop yield data from the RFA region reveals a large gap between the actual and water-limited yield. For example, for maize on average only 36 % of AY is actually realized under the current practices, suggesting that green water management practices should be combined with other measures that overcome the yield-reducing factors related to soil nutrient, tillage practices, plant protection, and cultivar improvement.

Finally, the CHC modeling framework developed in this study can be applied to conduct similar assessments in other regions. It can also be adopted for various agrometeorological applications, such as estimating seasonal water availability and crop water demand for both irrigated and rainfed systems, as well as predicting relative yields for the purpose of management planning. This framework minimizes dependence on process-based crop models for such analyses, which often require intensive measurement data for the calibration of several model parameters.

Data availability: The processed data and simulation output will be made available upon request.

Author contribution: Conceptualization: MTW; Data curation: MTW; Modelling and analysis: MTW; Methodological and result discussions: MTW, NP, JS, PM; Darft preparation: MTW; Revision: NP, JS, PM; Supervision: PM

Competing interests: At least one of the (co-)authors is a member of the editorial board of Hydrology and Earth System Sciences. The authors have no other competing interests.

Acknowledgments

We thank Silvan Ragettli for his valuable comments and suggestions on the evapotranspiration data and outputs. MTW was supported by ETH for Development (ETH4D), ETH Zurich, through the E4D Doctoral Scholarship Program. NP was supported by the Swiss National Science Foundation (SNSF), Grant 194649 (“Rainfall and floods in future cities”).

References

Abatzoglou, J. T., Dobrowski, S. Z., Parks, S. A. and Hegewisch, K. C.: Data Descriptor : TerraClimate , a high-resolution global dataset of monthly climate and climatic water balance from 1958 – 2015, , 1–12, 2017.

Abera, K., Crespo, O., Seid, J. and Mequanent, F.: Simulating the impact of climate change on maize production in Ethiopia, East Africa, Environ. Syst. Res., 7(1), doi:10.1186/s40068-018-0107-z, 2018.

Abrams, L.: Unlocking the potential of enhanced rainfed agriculture, Stockholm. [online] Available from: www.siwi.org/publications, 2018.

Adam, M., Van Bussel, L. G. J., Leffelaar, P. A., Van Keulen, H. and Ewert, F.: Effects of modelling detail on simulated

https://doi.org/10.5194/hess-2024-37
Preprint. Discussion started: 20 February 2024


Hydrology and Earth System Sciences
Discussions

potential crop yields under a wide range of climatic conditions, Ecol. Modell., 222(1), 131–143, doi:10.1016/j.ecolmodel.2010.09.001, 2011.

Allen, R. G., Pereira, L. S., Raes, D. and Smith, M.: Crop Evapotranspiration, Rome., 1998.

Anandhi, A., Frei, A., Pierson, D. C., Schneiderman, E. M., Zion, M. S., Lounsbury, D. and Matonse, A. H.: Examination of change factor methodologies for climate change impact assessment, , 47, 1–10, doi:10.1029/2010WR009104, 2011.

Araya, A., Stroosnijder, L., Girmay, G. and Keesstra, S. D.: Crop coefficient, yield response to water stress and water productivity of teff (Eragrostis tef (Zucc.), Agric. Water Manag., 98(5), 775–783, doi:10.1016/j.agwat.2010.12.001, 2011.

Araya, A., Girma, A. and Getachew, F.: Exploring Impacts of Climate Change on Maize Yield in Two Contrasting Agro-Ecologies of Ethiopia, Asian J. Appl. Sci. Eng., 4(10), 2305–915, 2015.

Borgomeo, E., Khan, H. F., Heino, M., Zaveri, E., Kummu, M., Brown, C. and Jägerskog, A.: Impact of green water anomalies on global rainfed crop yields, Environ. Res. Lett., 15(12), doi:10.1088/1748-9326/abc587, 2020.

Buchhorn, M., Smets, B., Bertels, L., De Roo, B., Lesiv, M. and Tsendbazar, Nandin-Erdene Tarko, A.: Copernicus Global Land Operations ”Vegetation and Energy” “CGLOPS-1,” Copernicus Glob. L. Oper., 1–93, doi:10.5281/zenodo.3938963.PU, 2020.

Budyko, M. I.: The Heat Balance of the Earth’s Surface, , 259, 1958.

Burke, M. B., Lobell, D. B. and Guarino, L.: Shifts in African crop climates by 2050, and the implications for crop improvement and genetic resources conservation, Glob. Environ. Chang., 19(3), 317–325, doi:10.1016/j.gloenvcha.2009.04.003, 2009.

Conway, D. and Vincent, K.: Conversations About Climate Risk, Adaptation and Resilience in Africa., 2021.

CSA: Summary and statistical report of the 2007 population and housing census, Addis Ababa. [online] Available from: https://www.statsethiopia.gov.et/census-2007-2/, 2007.

CSA: Agricultural sample survey (2010/2011): Report on area and production of crops, Addis Ababa, Ethiopia. [online] Available from: https://www.statsethiopia.gov.et/our-survey-reports/, 2010.

Degife, A. W., Zabel, F. and Mauser, W.: Climate change impacts on potential maize yields in Gambella Region, Ethiopia, Reg. Environ. Chang., 21(2), doi:10.1007/s10113-021-01773-3, 2021.

van Diepen, C. A., Wolf, J., van Keulen, H. and Rappoldt, C.: WOFOST: a simulation model of crop production, Soil Use Manag., 5(1), 16–24, doi:10.1111/j.1475-2743.1989.tb00755.x, 1989.

Dijk, M. Van, Morley, T., Jongeneel, R., Ittersum, M. Van, Reidsma, P. and Ruben, R.: Disentangling agronomic and economic yield gaps : An integrated framework and application, Agric. Syst., 154(February), 90–99,

580 doi:10.1016/j.agsy.2017.03.004, 2017.

Doorenbos, J. and Kassam, A. H.: Paper 33. Yield Response to water., 1979.

Falkenmark, M.: The New Blue and Green Water Paradigm : Breaking New Ground for Water Resources Planning and Management, , 132(June), 129–132, doi:10.1061/(ASCE)0733-9496(2006)132, 2006.

Fan, J., McConkey, B., Wang, H. and Janzen, H.: Root distribution by depth for temperate agricultural crops, F. Crop. Res.,
585 189, 68–74, doi:10.1016/j.fcr.2016.02.013, 2016.

FAO: Crops and climate change impact briefs. Climate-smart agriculture for more sustainable, resilient, and equitable food systems, Rome., 2022.

FDRE: Ethiopia's Climate Resilient Green Economy: National Adaptation Plan, Addis Ababa, Ethiopia., 2019.

Funk, C., Peterson, P., Landsfeld, M., Pedreros, D., Verdin, J., Shukla, S., Husak, G., Rowland, J., Harrison, L., Hoell, A. and
590 Michaelsen, J.: The climate hazards infrared precipitation with stations - A new environmental record for monitoring extremes, Nat. Sci. Data, 2, doi:10.1038/sdata.2015.66, 2015.

Grossi, A. and Dinku, T.: From research to practice: Adapting agriculture to climate today for tomorrow in Ethiopia, Front. Clim., doi:10.3389/fclim.2022.931514, 2022.

Hadgu, G., Tesfaye, K. and Mamo, G.: Analysis of climate change in Northern Ethiopia: implications for agricultural
595 production, Theor. Appl. Climatol., 121(3–4), 733–747, doi:10.1007/s00704-014-1261-5, 2015.

Hamby, D. .: A review of techniques for parameter sensitivity analysis of environmental models, Environ. Monit. Assess., 32, 135–154, doi:10.1007/BF00547132, 1994.

Hartmann, M. and Six, J.: Soil structure and microbiome functions in agroecosystems, Nat. Rev. Earth Environ., 4(1), 4–18, doi:10.1038/s43017-022-00366-w, 2023.

600 Hatfield, J. L. and Dold, C.: Water-use efficiency: Advances and challenges in a changing climate, Front. Plant Sci., 10(February), 1–14, doi:10.3389/fpls.2019.00103, 2019.

Hawkins, R. H., Moglen, G. E., Ward, T. J. and Woodward, D. E.: Watershed Management 2020 99, in Watershed Management 2020, pp. 301–340., 2020.

Holzworth, D. P., Huth, N. I., deVoil, P. G., Zurcher, E. J., Herrmann, N. I., McLean, G., Chenu, K., van Oosterom, E. J.,
605 Snow, V., Murphy, C., Moore, A. D., Brown, H., Whish, J. P. M., Verrall, S., Fainges, J., Bell, L. W., Peake, A. S., Poulton, P. L., Hochman, Z., Thorburn, P. J., Gaydon, D. S., Dalgliesh, N. P., Rodriguez, D., Cox, H., Chapman, S., Doherty, A., Teixeira, E., Sharp, J., Cichota, R., Vogeler, I., Li, F. Y., Wang, E., Hammer, G. L., Robertson, M. J., Dimes, J. P., Whitbread, A. M., Hunt, J., van Rees, H., McClelland, T., Carberry, P. S., Hargreaves, J. N. G., MacLeod, N.,

https://doi.org/10.5194/hess-2024-37
Preprint. Discussion started: 20 February 2024


Hydrology and Earth System Sciences Discussions

McDonald, C., Harsdorf, J., Wedgwood, S. and Keating, B. A.: APSIM - Evolution towards a new generation of agricultural systems simulation, Environ. Model. Softw., 62, 327–350, doi:10.1016/j.envsoft.2014.07.009, 2014.

Hurni, H.: Soil and Water Conservation in Ethiopia: Guidlines for Development Agents, Bern Open Publishing (BOP)., 2016.

IFPRI and CSA: Atlas of the Ethiopian Rural Economy, International Food Policy Research Institute, Washinton DC., 2006.

Iglesias, A. and Garrote, L.: Adaptation strategies for agricultural water management under climate change in Europe, Agric. Water Manag., 155, 113–124, doi:10.1016/j.agwat.2015.03.014, 2015.

van Ittersum, M. K., Cassman, K. G., Grassini, P., Wolf, J., Tittonell, P. and Hochman, Z.: Yield gap analysis with local to global relevance-A review, F. Crop. Res., 143, 4–17, doi:10.1016/j.fcr.2012.09.009, 2013.

Jägermeyr, J., Müller, C., Ruane, A. C., Elliott, J., Balkovic, J., Castillo, O., Faye, B., Foster, I., Folberth, C., Franke, J. A., Fuchs, K., Guarin, J. R., Heinke, J., Hoogenboom, G., Iizumi, T., Jain, A. K., Kelly, D., Khabarov, N., Lange, S., Lin, T. S., Liu, W., Mialyk, O., Minoli, S., Moyer, E. J., Okada, M., Phillips, M., Porter, C., Rabin, S. S., Scheer, C., Schneider, J. M., Schyns, J. F., Skalsky, R., Smerald, A., Stella, T., Stephens, H., Webber, H., Zabel, F. and Rosenzweig, C.: Climate impacts on global agriculture emerge earlier in new generation of climate and crop models, Nat. Food, 2(11), 873–885, doi:10.1038/s43016-021-00400-y, 2021.

Jones, J. W., Hoogenboom, G., Porter, C. H., Boote, K. J., Batchelor, W. D., Hunt, L. A., Wilkens, P. W., Singh, U., Gijsman, A. J. and Ritchie, J. T.: The DSSAT cropping system model., 2003.

Kang, Y., Khan, S. and Ma, X.: Climate change impacts on crop yield, crop water productivity and food security - A review, Prog. Nat. Sci., 19(12), 1665–1674, doi:10.1016/j.pnsc.2009.08.001, 2009.

Kassawmar, T., Zeleke, G., Bantider, A., Gessesse, G. D. and Abraha, L.: A synoptic land change assessment of Ethiopia's Rainfed Agricultural Area for evidence-based agricultural ecosystem management, Heliyon, 4(11), e00914, doi:10.1016/j.heliyon.2018.e00914, 2018.

Kassawmar, T., Zeleke, G., Bantider, A., Gessesse, G. D., Abebe, S., Abraha, L. and Tadesse, M.: State of cropland availability in rainfed farming systems in Ethiopia: Alternative pathways to address landlessness and food insecurity. In: Ethiopia: Social and Political Issues, in Ethiopia: Social and Political Issues, vol. 1, pp. 228–260, NOVA., 2019.

Kassie, B. T., Rötter, R. P., Hengsdijk, H., Asseng, S., Van Ittersum, M. K., Kahiluoto, H. and Van Keulen, H.: Climate variability and change in the Central Rift Valley of Ethiopia: Challenges for rainfed crop production, J. Agric. Sci., 152(1), 58–74, doi:10.1017/S0021859612000986, 2014.

Kukal, M. S. and Irmak, S.: Climate-Driven Crop Yield and Yield Variability and Climate Change Impacts on the U.S. Great Plains Agricultural Production, Nat. Sci. Rep., 8(8), 1–18, doi:10.1038/s41598-018-21848-2, 2018.

Kummu, M., Heino, M., Taka, M., Varis, O. and Viviroli, D.: Climate change risks pushing one-third of global food production

outside the safe climatic space, One Earth, 4(5), 720–729, doi:10.1016/j.oneear.2021.04.017, 2021.

Laderach, P., Ramirez-Villegas, J., Prager, S. D., Osorio, D., Krendelsberger, A., Zougmore, R. B., Charbonneau, B., Van Dijk, H., Madurga-Lopez, I. and Pacillo, G.: The importance of food systems in a climate crisis for peace and security in the Sahel, Int. Rev. Red Cross, 103(918), 995–1028, doi:10.1017/S1816383122000170, 2021.

Lala, J., Yang, M., Wang, G. and Block, P.: Utilizing rainy season onset predictions to enhance maize yields in Ethiopia, Environ. Res. Lett., 16(5), doi:10.1088/1748-9326/abf9c9, 2021.

Liu, M., Wang, D., Chen, X., Chen, Y., Gao, L. and Deng, H.: Impacts of climate variability and land use on the blue and green water resources in a subtropical basin of China, Sci. Rep., 12(1), 1–11, doi:10.1038/s41598-022-21880-3, 2022a.

Liu, X., Liu, W., Tang, Q., Liu, B., Wada, Y. and Yang, H.: Global Agricultural Water Scarcity Assessment Incorporating Blue and Green Water Availability Under Future Climate Change, Earth's Futur., 10(4), doi:10.1029/2021EF002567, 2022b.

Lobell, D. B., Cassman, K. G. and Field, C. B.: Crop yield gaps: Their importance, magnitudes, and causes, Annu. Rev. Environ. Resour., 34, 179–204, doi:10.1146/annurev.environ.041008.093740, 2009.

Lobell, D. B., Schlenker, W. and Costa-Roberts, J.: Climate Trends and Global crop production since 1980 1980, , 333(June), 1186–1189, doi:10.1126/science.1206376, 2011.

Makurira, H., Savenije, H. H. G., Uhlenbrook, S., Rockström, J. and Senzanje, A.: Investigating the water balance of on-farm techniques for improved crop productivity in rainfed systems: A case study of Makanya catchment, Tanzania, Phys. Chem. Earth, 34(1–2), 93–98, doi:10.1016/j.pce.2008.04.003, 2009.

Manik, S. M. N., Pengilley, G., Dean, G., Field, B., Shabala, S. and Zhou, M.: Soil and crop management practices to minimize the impact of waterlogging on crop productivity, Front. Plant Sci., 10(February), 1–23, doi:10.3389/fpls.2019.00140, 2019.

Markos, D., Worku, W. and Mamo, G.: Exploring adaptation responses of maize to climate change scenarios in southern central Rift Valley of Ethiopia, Sci. Rep., 13(1), 1–18, doi:10.1038/s41598-023-39795-y, 2023.

Meinshausen, M., Nicholls, Z. R. J., Lewis, J., Gidden, M. J., Vogel, E., Freund, M., Beyerle, U., Gessner, C., Nauels, A., Bauer, N., Canadell, J. G., Daniel, J. S., John, A., Krummel, P. B., Luderer, G., Meinshausen, N., Montzka, S. A., Rayner, P. J., Reimann, S., Smith, S. J., Van Den Berg, M., Velders, G. J. M., Vollmer, M. K. and Wang, R. H. J.: The shared socio-economic pathway (SSP) greenhouse gas concentrations and their extensions to 2500, Geosci. Model Dev., 13(8), 3571–3605, doi:10.5194/gmd-13-3571-2020, 2020.

Mekonnen, M. M. and Hoekstra, A. Y.: The green, blue and grey water footprint of crops and derived crop products, Hydrol. Earth Syst. Sci., 15(5), 1577–1600, doi:10.5194/hess-15-1577-2011, 2011.

https://doi.org/10.5194/hess-2024-37
Preprint. Discussion started: 20 February 2024

Meng, M., Pu, X., Li, S., Zhang, Y., Wang, J., Xu, H., Hu, Y., Wang, J. and Wang, Y.: Sensitivities of rainfed maize production to root zone soil water , air temperature and shortwave radiation in the Sanjiang Plain under sub- humid cool-temperate climates, Water-Energy Nexus, 6, 131–136, doi:10.1016/j.wen.2023.09.003, 2023.

Moges, D. M. and Gangadhara, B. H.: Climate change and its implications for rainfed agriculture in Ethiopia, J. Water Clim. Chang., 12(4), 1229–1244, doi:10.2166/wcc.2020.058, 2021.

Mohammadi, S., Rydgren, K., Bakkestuen, V. and Gillespie, M. A. K.: Impacts of recent climate change on crop yield can depend on local conditions in climatically diverse regions of Norway, Sci. Rep., 13(1), 1–12, doi:10.1038/s41598-023-30813-7, 2023.

Molden, D., Vithanage, M., de Fraiture, C., Faures, J. M., Gordon, L., Molle, F. and Peden, D.: Water Availability and Its Use in Agriculture, Treatise Water Sci., 4, 707–732, doi:10.1016/B978-0-444-53199-5.00108-1, 2011.

Mthandi, J., Kahimba, F. C., Tarimo, A. K. P. R., Salim, B. A. and Lowole, M. W.: Root zone soil moisture redistribution in maize (<i>Zea mays</i> L.) under different water application regimes, Agric. Sci., 04(10), 521–528, doi:10.4236/as.2013.410070, 2013.

Mu, Q., Zhao, M. and Running, S. W.: MODIS Global Terrestrial Evapotranspiration (ET) Product (NASA MOD16A2/A3) Algorithm Theoretical Basis Document Collection 5, , (March), 1–40, 2019.

Müller, C., Cramer, W., Hare, W. L. and Lotze-Campen, H.: Climate change risks for African agriculture, Proc. Natl. Acad. Sci. U. S. A., 108(11), 4313–4315, doi:10.1073/pnas.1015078108, 2011.

Muñoz-Sabater, J., Dutra, E., Agustí-Panareda, A., Albergel, C., Arduini, G., Balsamo, G., Boussetta, S., Choulga, M., Harrigan, S., Hersbach, H., Martens, B., Miralles, D. G., Piles, M. M., Rodríguez-Fernández, N. J., Zsoter, E., Buontempo, C. and Thépaut, J.-N. N.: ERA5-Land: A state-of-the-art global reanalysis dataset for land applications, Earth Syst. Sci. Data, 13(9), 4349–4383, doi:10.5194/essd-13-4349-2021, 2021.

Nash, J. E. and Sutcliffe, J. V.: River flow forecasting through conceptual models part I - A discussion of principles, J. Hydrol., 10(3), 282–290, doi:10.1016/0022-1694(70)90255-6, 1970.

Nyakudya, I. W., Stroosnijder, L. and Nyagumbo, I.: Infiltration and planting pits for improved water management and maize yield in semi-arid Zimbabwe, Agric. Water Manag., 141, 30–46, doi:10.1016/j.agwat.2014.04.010, 2014.

O'Neill, B. C., Tebaldi, C., Van Vuuren, D. P., Eyring, V., Friedlingstein, P., Hurtt, G., Knutti, R., Kriegler, E., Lamarque, J. F., Lowe, J., Meehl, G. A., Moss, R., Riahi, K. and Sanderson, B. M.: The Scenario Model Intercomparison Project (ScenarioMIP) for CMIP6, Geosci. Model Dev., 9(9), 3461–3482, doi:10.5194/gmd-9-3461-2016, 2016.

Park, S., Chun, J. A., Kim, D. and Sitthikone, M.: Climate risk management for the rainfed rice yield in Lao PDR using APCC MME seasonal forecasts, Agric. Water Manag., 274(October), 107976, doi:10.1016/j.agwat.2022.107976, 2022.

https://doi.org/10.5194/hess-2024-37
Preprint. Discussion started: 20 February 2024

Peleg, N., Molnar, P., Burlando, P. and Fatichi, S.: Exploring stochastic climate uncertainty in space and time using a gridded hourly weather generator, J. Hydrol., 571(February), 627–641, doi:10.1016/j.jhydrol.2019.02.010, 2019.

Pittelkow, C. M., Linquist, B. A., Lundy, M. E., Liang, X., van Groenigen, K. J., Lee, J., van Gestel, N., Six, J., Venterea, R. T. and van Kessel, C.: When does no-till yield more? A global meta-analysis, F. Crop. Res., 183, 156–168, doi:10.1016/j.fcr.2015.07.020, 2015.

Poggio, L., De Sousa, L. M., Batjes, N. H., Heuvelink, G. B. M., Kempen, B., Ribeiro, E. and Rossiter, D.: SoilGrids 2.0: Producing soil information for the globe with quantified spatial uncertainty, Soil, 7(1), 217–240, doi:10.5194/soil-7-217-2021, 2021.

Raes, D., Steduto, P., Hsiao, T. C. and Fereres, E.: Aquacrop-The FAO crop model to simulate yield response to water: II. main algorithms and software description, Agron. J., 101(3), 438–447, doi:10.2134/agronj2008.0140s, 2009.

Raes, D., Steduto, P., Hsiao, T. C. and Fereres, E.: AquaCrop Version 7.1 Reference manual, Rome., 2022.

Ramirez-Villegas, J., Koehler, A. K. and Challinor, A. J.: Assessing uncertainty and complexity in regional-scale crop model simulations, Eur. J. Agron., 88, 84–95, doi:10.1016/j.eja.2015.11.021, 2017.

Rezaei, E. E., Webber, H., Asseng, S., Boote, K., Durand, J. L., Ewert, F., Martre, P. and MacCarthy, D. S.: Climate change impacts on crop yields, Nat. Rev. Earth Environ., 4(December), 16, doi:10.1038/s43017-023-00491-0, 2023.

Ringersma, J., Batjes, N. and Dent, D.: Green Water: definitions and data for assessment. [online] Available from: http://www.isric.org/isric/webdocs/docs/ISRICGreenwater ReviewFebr2004_.pdf, 2003.

Rockström, J.: On-farm green water estimates as a tool for increased food production in water scarce regions, Phys. Chem. Earth, Part B Hydrol. Ocean. Atmos., 24(4), 375–383, doi:10.1016/S1464-1909(99)00016-7, 1999.

Rockström, J.: Water for food and nature in drought-prone tropics: Vapour shift in rain-fed agriculture, Philos. Trans. R. Soc. B Biol. Sci., 358(1440), 1997–2009, doi:10.1098/rstb.2003.1400, 2003.

Rockström, J. and Gordon, L.: Assessment of Green Water Flows to Sustain Major Biomes of the World: Implications for Future Ecohydrological Landscape Management, Phys. Chem. Earth, Part B Hydrol. Ocean. Atmos., 26(11–12), 843–851, doi:10.1016/S1464-1909(01)00096-X, 2001.

Rockström, J., Karlberg, L., Wani, S. P., Barron, J., Hatibu, N., Oweis, T., Bruggeman, A., Farahani, J. and Qiang, Z.: Managing water in rainfed agriculture-The need for a paradigm shift, Agric. Water Manag., 97(4), 543–550, doi:10.1016/j.agwat.2009.09.009, 2010.

Rosenzweig, C., Elliott, J., Deryng, D., Ruane, A. C., Müller, C., Arneth, A., Boote, K. J., Folberth, C., Glotter, M., Khabarov, N., Neumann, K., Piontek, F., Pugh, T. A. M., Schmid, E., Stehfest, E., Yang, H. and Jones, J. W.: Assessing agricultural risks of climate change in the 21st century in a global gridded crop model intercomparison, Proc. Natl. Acad. Sci. U. S.

https://doi.org/10.5194/hess-2024-37
Preprint. Discussion started: 20 February 2024

A., 111(9), 3268–3273, doi:10.1073/pnas.1222463110, 2014.

Ross, C. W., Prihodko, L., Anchang, J., Kumar, S., Ji, W. and Hanan, N. P.: HYSOGs250m, global gridded hydrologic soil groups for curve-number-based runoff modeling, Sci. data, 5, 180091, doi:10.1038/sdata.2018.91, 2018.

Rui, H. L. and Beaudoing, H.: README Document for NASA GLDAS Version 2 Data Products, Goddard Earth Sci. Data Inf. Serv. Cent. (GES DISC), 16(1), 1–32 [online] Available from: https://hydro1.gesdisc.eosdis.nasa.gov/data/GLDAS/README_GLDAS2.pdf, 2020.

Saxton, K. E. and Rawls, W. J.: Soil Water Characteristic Estimates by Texture and Organic Matter for Hydrologic Solutions, Soil Sci. Soc. Am. J., 70(5), 1569–1578, doi:10.2136/sssaj2005.0117, 2006.

Schlenker, W. and Lobell, D. B.: Robust negative impacts of climate change on African agriculture, Environ. Res. Lett., 5(1), doi:10.1088/1748-9326/5/1/014010, 2010.

Schuol, J., Abbaspour, K. C., Yang, H., Srinivasan, R. and Zehnder, A. J. B.: Modeling blue and green water availability in Africa, Water Resour. Res., 44(7), 1–18, doi:10.1029/2007WR006609, 2008.

Segele, Z. T. and Lamb, P. J.: Characterization and variability of Kiremt rainy season over Ethiopia, Meteorol. Atmos. Phys., 89(1–4), 153–180, doi:10.1007/s00703-005-0127-x, 2005.

Senay, G. B., Kagone, S. and Velpuri, N. M.: Operational Global Actual Evapotranspiration :, Sensors, (Vic), 1–18, 2020.

Siad, S. M., Iacobellis, V., Zdruli, P., Gioia, A., Stavi, I. and Hoogenboom, G.: A review of coupled hydrologic and crop growth models, Agric. Water Manag., 224(June), 105746, doi:10.1016/j.agwat.2019.105746, 2019.

Smedema, L. K. and Rycroft, D. W.: Land drainage: planning and design of agricultural drainage systems., , 0, 183–184, doi:10.1016/0378-3774(85)90006-x, 1983.

Spinoni, J., Vogt, J., Naumann, G., Carrao, H. and Barbosa, P.: Towards identifying areas at climatological risk of desertification using the Köppen-Geiger classification and FAO aridity index, Int. J. Climatol., 35(9), 2210–2222, doi:10.1002/joc.4124, 2015.

Sposito, G.: Green Water and Global Food Security, Vadose Zo. J., 12(4), 1–6, doi:10.2136/vzj2013.02.0041, 2013.

Steduto, P., Hsiao, T. C., Raes, D. and Fereres, E.: Aquacrop-the FAO crop model to simulate yield response to water: I. concepts and underlying principles, Agron. J., 101(3), 426–437, doi:10.2134/agronj2008.0139s, 2009.

Steduto, P., Hsiao, T. C., Fereres, E. and Raes, D.: Crop yield response to water. [online] Available from: https://www.fao.org/3/i2800e/i2800e.pdf (Accessed 7 October 2023), 2012.

Stöckle, C. O., Donatelli, M. and Nelson, R.: CropSyst, a cropping systems simulation model, Eur. J. Agron., 18(3–4), 289–307, doi:10.1016/S1161-0301(02)00109-0, 2003.

https://doi.org/10.5194/hess-2024-37
Preprint. Discussion started: 20 February 2024


Hydrology and Earth System Sciences
Discussions

Teutschbein, C. and Seibert, J.: Bias correction of regional climate model simulations for hydrological climate-change impact studies: Review and evaluation of different methods, J. Hydrol., 456–457, 12–29, doi:10.1016/j.jhydrol.2012.05.052, 2012.

Tittonell, P. and Giller, K. E.: When yield gaps are poverty traps: The paradigm of ecological intensification in African smallholder agriculture, F. Crop. Res., 143, 76–90, doi:10.1016/j.fcr.2012.10.007, 2013.

UNFCCC: Progress in the Formulation and Implementation of Naps, 2021.

USDA: Urban Hydrology for Small Watersheds. [online] Available from: http://scholar.google.com/scholar?hl=en&btnG=Search&q=intitle:Urban+Hydrology+for+Small+watersheds#1, 1985.

Wakjira, M. T., Peleg, N., Anghileri, D., Molnar, D., Alamirew, T., Six, J. and Molnar, P.: Rainfall seasonality and timing: implications for cereal crop production in Ethiopia, Agric. For. Meteorol., 310, 108633, doi:10.1016/J.AGRFORMET.2021.108633, 2021.

Wakjira, M. T., Peleg, N., Molnar, P. and Burlando, P.: Bias-corrected and downscaled ERA5-Land 2-m air temperature dataset for Ethiopia for the period 1981-2010., 2022.

Wakjira, M. T., Peleg, N., Burlando, P. and Molnar, P.: Gridded daily 2-m air temperature dataset for Ethiopia derived by debiasing and downscaling ERA5-Land for the period 1981–2010, Data Br., 46, 108844, doi:10.1016/j.dib.2022.108844, 2023.

Warren, R. F., Wilby, R. L., Brown, K., Watkiss, P., Betts, R. A., Murphy, J. M. and Lowe, J. A.: Advancing national climate change risk assessment to deliver national adaptation plans, Philos. Trans. R. Soc. A Math. Phys. Eng. Sci., 376(2121), doi:10.1098/rsta.2017.0295, 2018.

Williams, J. .: The erosion-productivity impact calculator (EPIC) model: a case history, Philos. Trans. R. Soc. London. Ser. B Biol. Sci., 329(1255), 421–428, doi:10.1098/rstb.1990.0184, 1990.

Zhang, Y., Kong, D., Gan, R., Chiew, F. H. S., McVicar, T. R., Zhang, Q. and Yang, Y.: Coupled estimation of 500 m and 8-day resolution global evapotranspiration and gross primary production in 2002–2017, Remote Sens. Environ., 222(May 2018), 165–182, doi:10.1016/j.rse.2018.12.031, 2019.